ミクロなプラズマ素過程に基づく衝撃波粒子加速機構

Shock Acceleration Mechanisms Based on Microscopic Plasma Physical Processes

天野孝伸 (東京大学)
Takanobu Amano (U-Tokyo)

Collaborators
T. Katou, M. Hoshino (U-Tokyo), Y. Matsumoto (Chiba U), M. Oka (UCB), S. Matsukiyo (Kyusyu U) O. Kobzar (Jagiellonian U), J. Niemiec (INP/PAS), A. Bohdan M. Pohl (DESY)

Non-thermal Particles

Highly energetic charged particles with energies much larger than the thermal energy are ubiquitous in many astrophysical phenomena. The energy density of the non-thermal populations can be comparable to the thermal component.

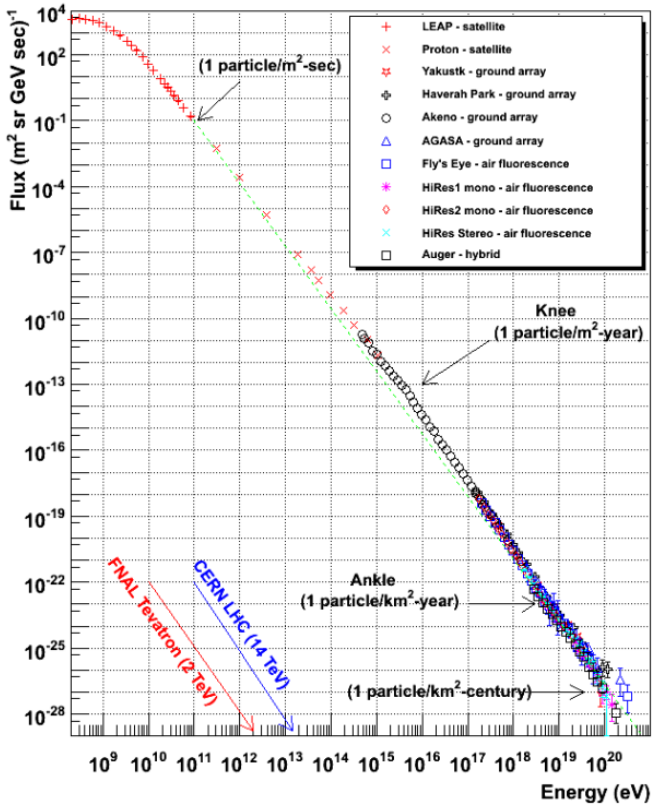

Blasi (2013), Amato (2014)

solar flare

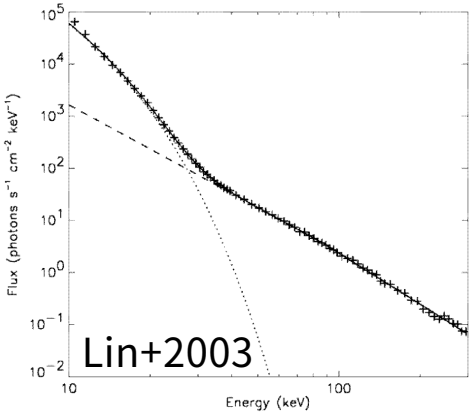

Earth bow shock

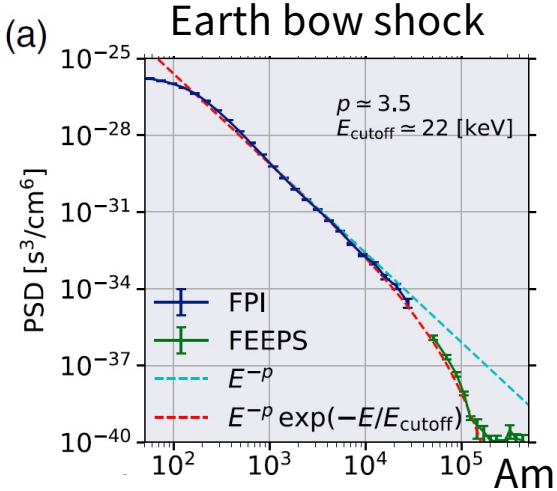

Amano+2020

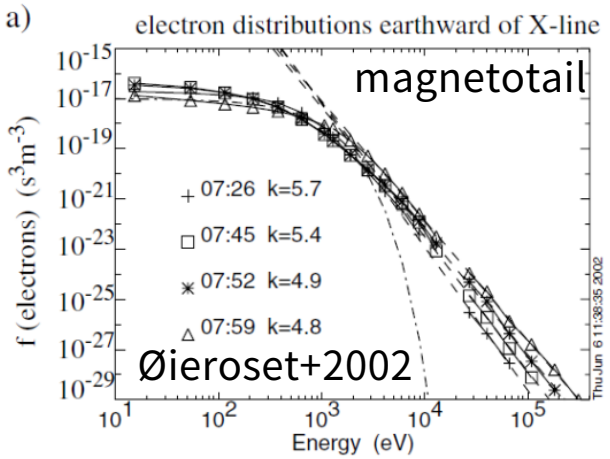

Fundamental Question: Energy Partition

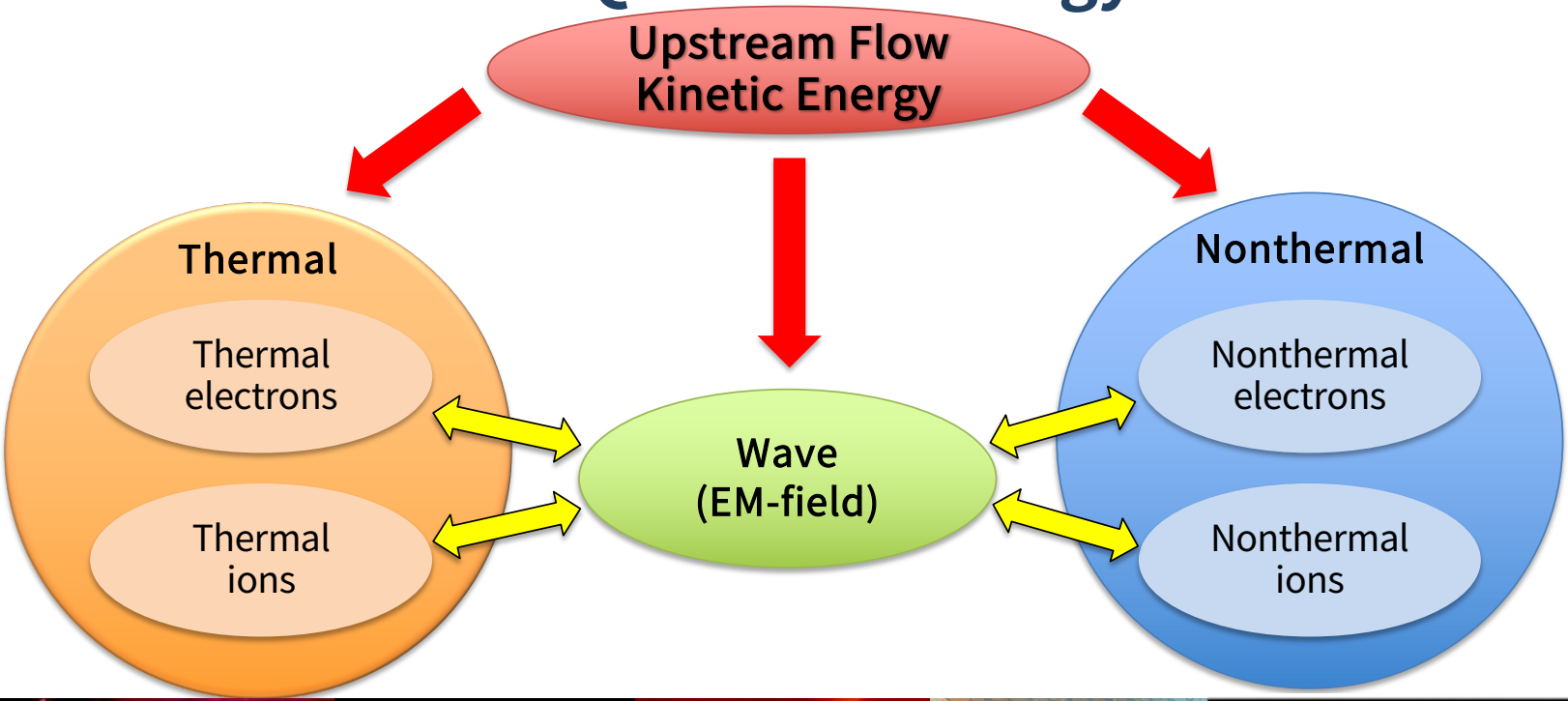

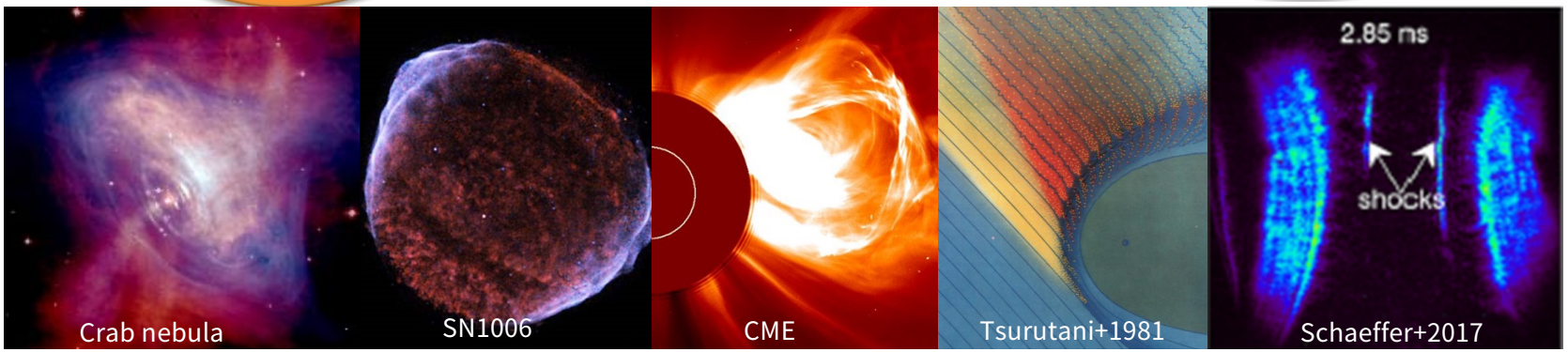

Standard Shock Acceleration Theory

- Diffusive Shock Acceleration (DSA)
  - A simple yet powerful model that predicts a nearly universal power-law; $N(E) \propto E^{-2}$

[e.g., Bell 1978, Blandford & Ostriker 1978]

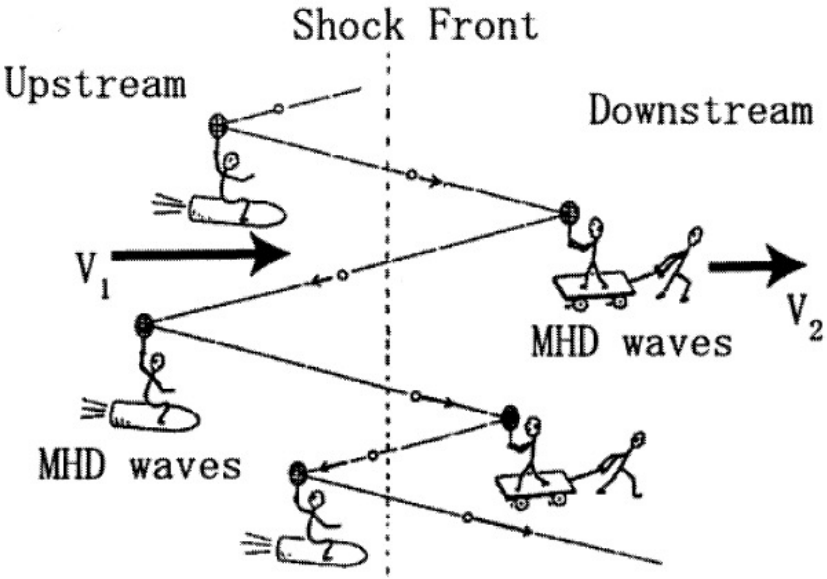

M. Scholer

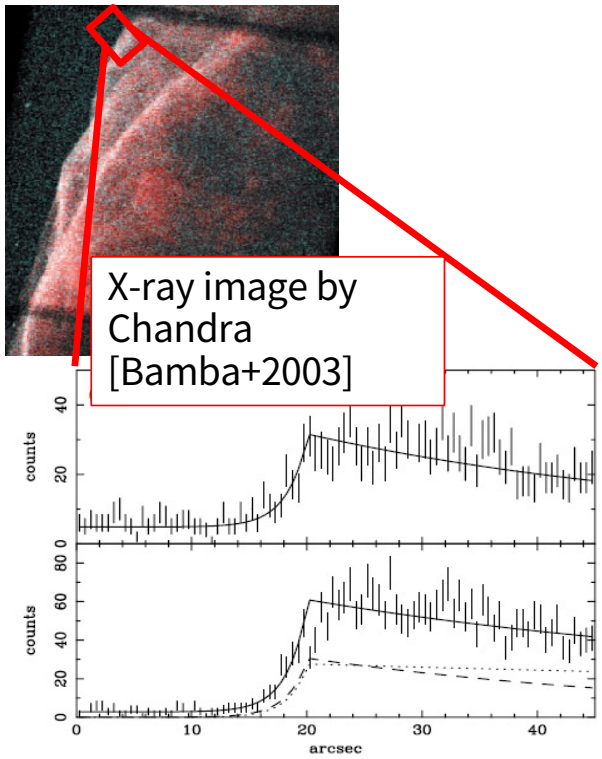

X-ray image by Chandra [Bamba+2003]

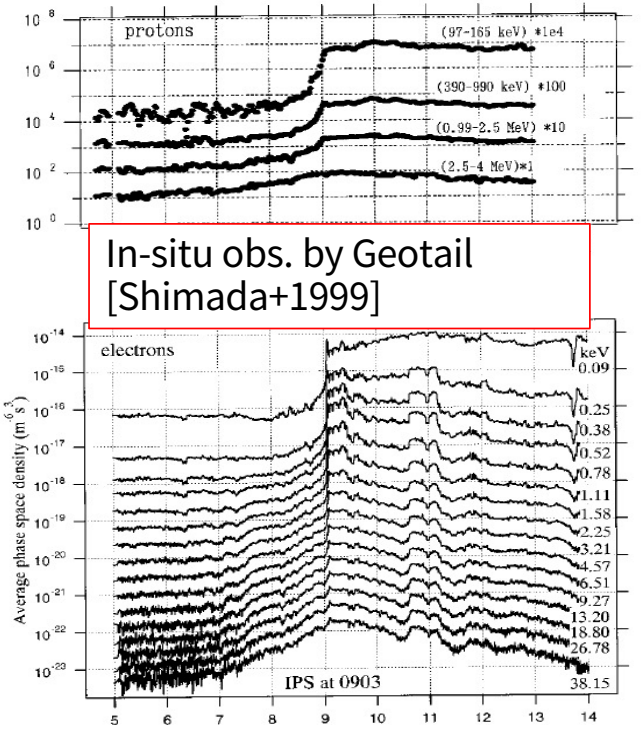

In-situ obs. by Geotail [Shimada+1999]

Diffusive Shock Acceleration

Consider the steady-state solution ($\partial/\partial t = 0$)for the following equation at a plane shock:

$$\frac{\partial f}{\partial t} + V\frac{\partial f}{\partial x} - \frac{1}{3}\frac{\partial V}{\partial x}\frac{\partial f}{\partial \ln p} = \frac{\partial}{\partial x}\left(\kappa\frac{\partial f}{\partial x}\right)$$

with a discontinuous flow profile

$$V(x) = \begin{cases} V_1 & x < 0 \\ V_2 & 0 < x \end{cases}, \qquad \frac{\partial V}{\partial x} = (V_2 - V_1)\delta(x).$$

The analytic solutions in the upstream and downstream (where $\partial V/\partial x = 0$) are given by

$$f(x,p) = \begin{cases} f_0(p)\exp\left(\frac{x}{\kappa_1/V_1}\right) & x < 0 \\ f_0(p) & 0 < x \end{cases},$$

where we have assumed the boundary condition: $f(x) = 0$ at $x \to -\infty$ and $\partial f/\partial x = 0$ at $x \to +\infty$.

Diffusive Shock Acceleration

The unknown $f_0(p)$ must be determined by connecting the two solutions at the shock using an appropriate boundary condition. This can be found by integrating the equation across the shock:

$$0 = \int_{-\epsilon}^{+\epsilon} \left[V\frac{\partial f}{\partial x} - \frac{1}{3}\frac{\partial V}{\partial x}\frac{\partial f}{\partial \ln p} - \frac{\partial}{\partial x}\left(\kappa \frac{\partial f}{\partial x}\right)\right] dx = \frac{V_1 - V_2}{3}\frac{\partial f}{\partial \ln p} - \left[\kappa \frac{\partial f}{\partial x}\right]_{-\epsilon}^{+\epsilon}$$
$$= \frac{V_1 - V_2}{3}\frac{\partial f_0}{\partial \ln p} + V_1 f_0(p).$$

In the last expression, we have substituted $(\kappa \partial f/\partial x)|_{x=-\epsilon} = V_1 f_0(p)$ and $(\kappa \partial f/\partial x)|_{x=+\epsilon} = 0$.

The solution is given by the power-law:

$$f_0(p) \propto p^{-q}, \quad q = \frac{3V_1}{V_1 - V_2} = \frac{3r}{r-1}$$

For relativistic particles $E \approx pc$,

$$N(E) = 4\pi p^2 f(p) \propto p^{-q+2} \propto E^{-(r+2)/(r-1)},$$

which agrees with the result obtained with the single particle approach.

reflected (field-aligned) ions

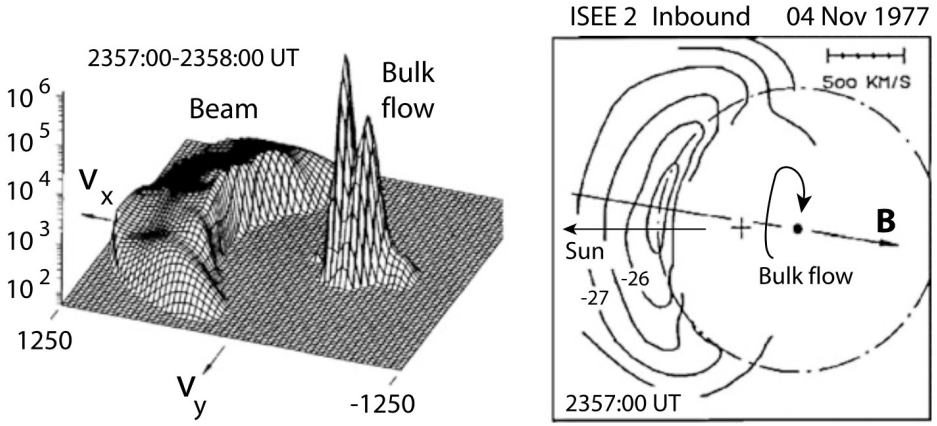

diffuse ions

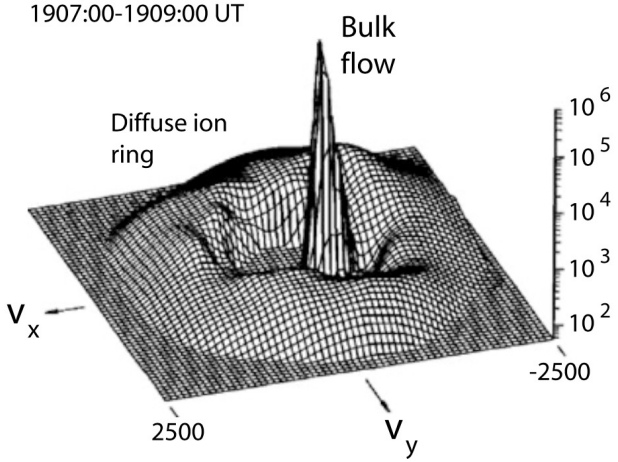

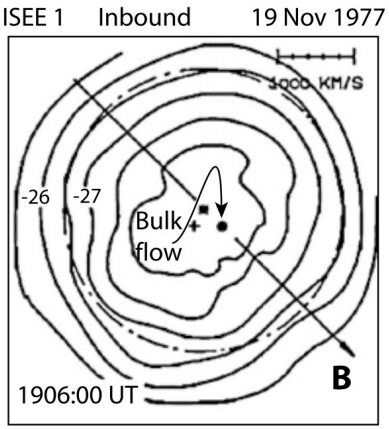

Balogh and Treumann

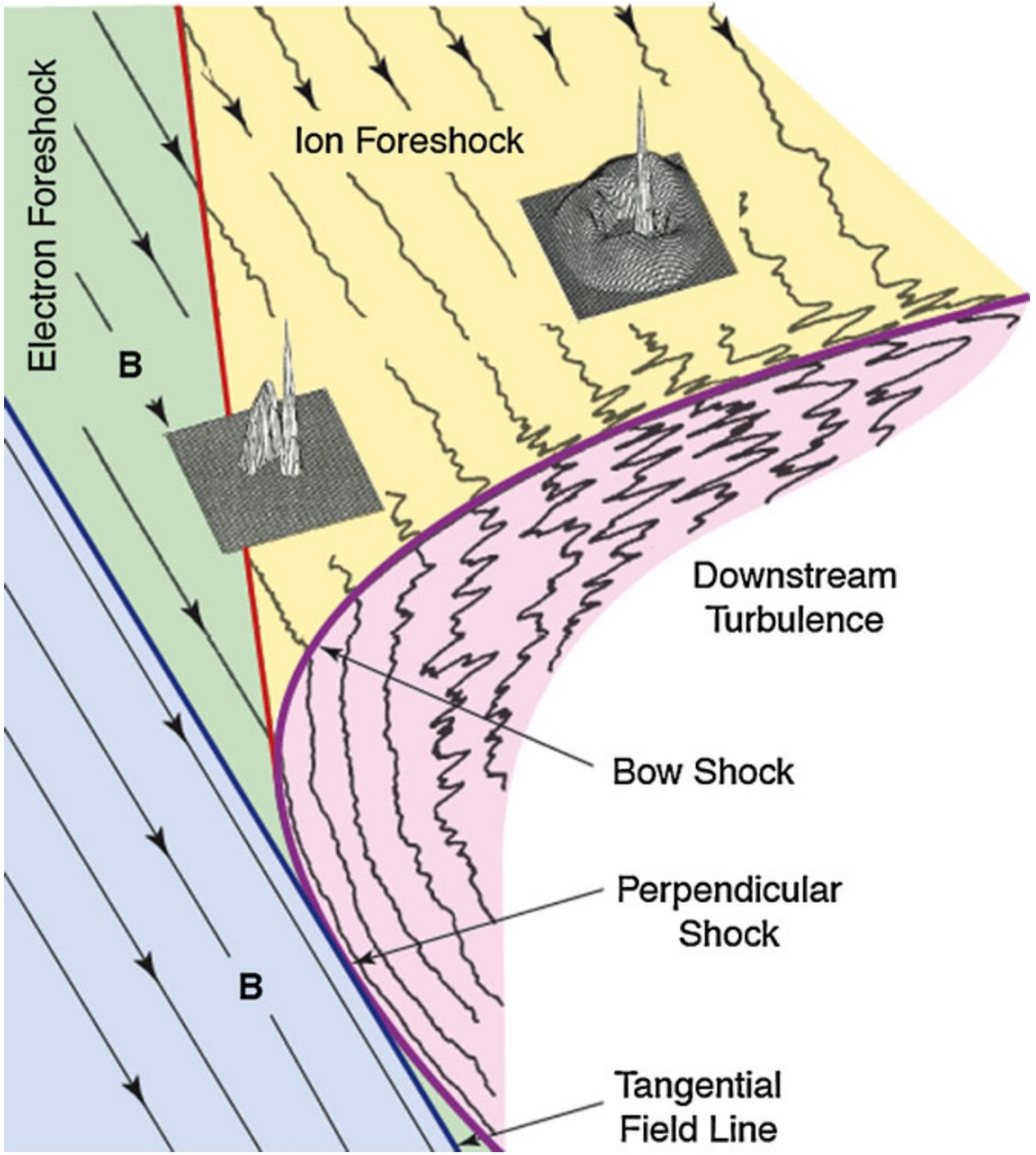

Ref: Jokipii (1987)

Diffusive Shock Acceleration at Oblique Shock

Acceleration rate relative to the parallel shock

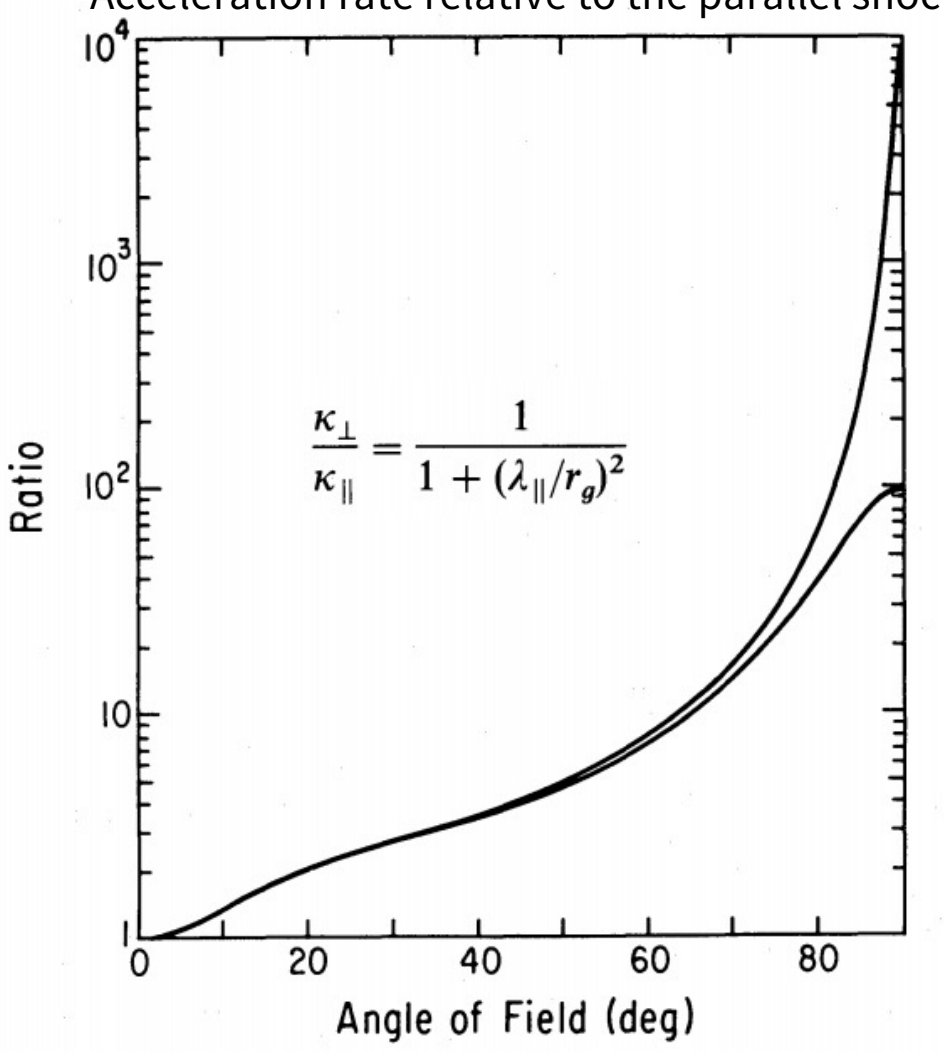

- While the spectral index does not change, quasi-perpendicular shocks can be much more efficient than quasi-parallel shocks in terms acceleration time.
- The diffusion approximation will breakdown when the shock is very close to purely perpendicular shock.
  [cf., Kirk & Schneider 1987, Takamoto & Kirk 2015]

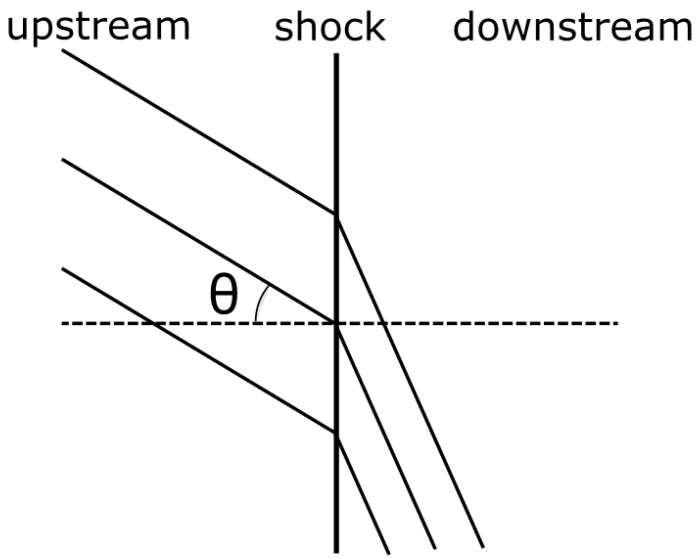

Ref: Drury (1983)

Diffusive Shock Acceleration at Oblique Shock

Spectral Index

Since the flow is everywhere parallel to the B-field in HTF, there is no energy by the convection electric field $E = -\frac{V}{c} \times B$. We may thus use the diffusion-convection equation of the following form:

$$\frac{\partial f}{\partial t} + V_x \frac{\partial f}{\partial x} - \frac{1}{3} \frac{\partial V_x}{\partial x} \frac{\partial f}{\partial \ln p} = \frac{\partial}{\partial x} \left(\kappa_{xx} \frac{\partial f}{\partial x} \right)$$

where $V_x = V \cos\theta$ and $\kappa_{xx} = \kappa_{\parallel} \cos^2\theta + \kappa_{\perp} \sin^2\theta$. Note that V is the field-aligned flow.

This indicates that the spectral index does not depend on the shock obliquity as long as $V/v \ll 1$ is satisfied !

Acceleration Time

The acceleration time is given by

$$\tau_{\rm acc}(p) = \frac{3}{V_{x,1} - V_{x,2}} \int_{p_0}^{p} dp' \left(\frac{\kappa_{1,xx}}{V_{x,1}} + \frac{\kappa_{2,xx}}{V_{x,2}} \right) \sim O\left(\frac{\kappa_{xx}}{V_x^2} \right),$$

which is proportional to the diffusion length *parallel to the shock normal*.

Ref: Wu (1984), Leroy & Mangeney (1984)

Shock Drift Acceleration (SDA)

- Since the energy is conserved in HTF, a particle with a sufficiently high pitch angle may secularly reflected back by the shock, which works as a moving magnetic mirror.
- The reflection predicts a momentum gain of $\Delta p \approx 2mV_0/\cos\theta_{Bn}$ as measured in the upstream frame.
- The adiabatic approximation is known to be adequate in an averaged sense even for a particle with the gyroradius much larger than the shock thickness [e.g., Terasawa 1979].

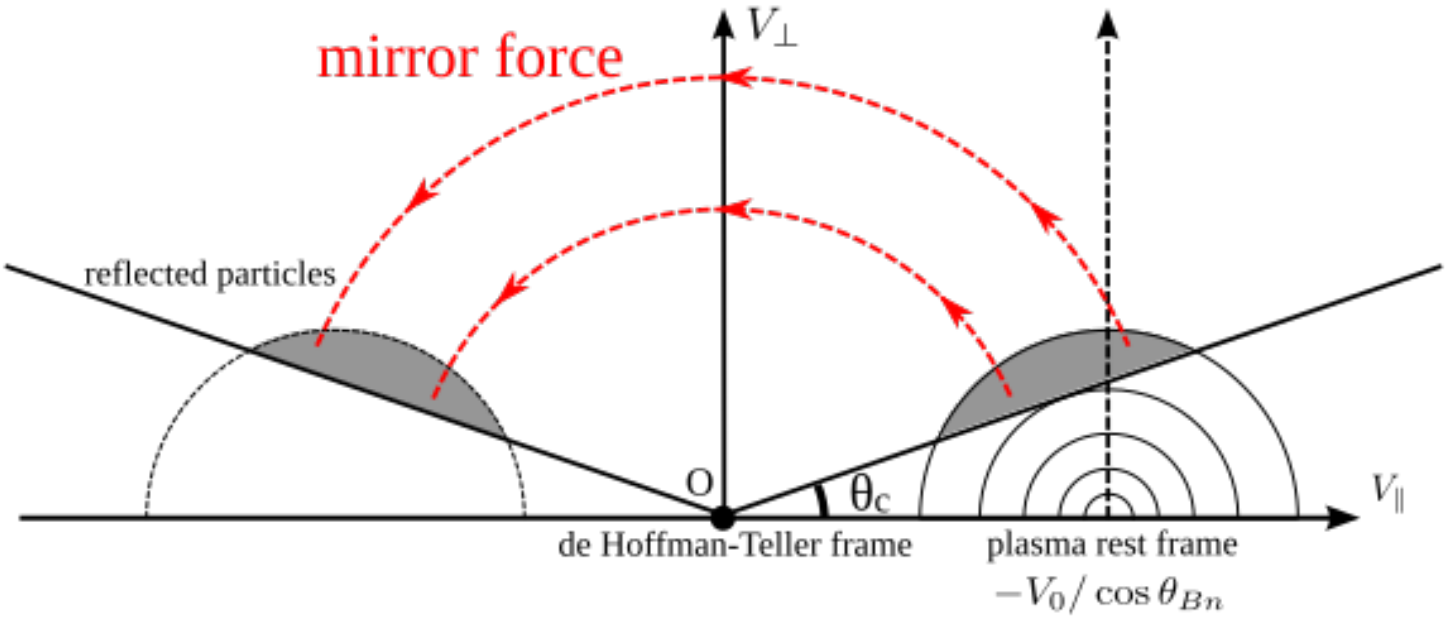

Ref: Decker (1988)

Diffusive Shock Acceleration at Oblique Shock

The energy gain term may be decomposed as

$$\frac{\partial V_x}{\partial x} = -V_x \left(\frac{\partial \ln B}{\partial x} - \frac{\partial \ln V}{\partial x} \right),$$

which indicates SDA and first-order Fermi acceleration both contributes the energy gain.

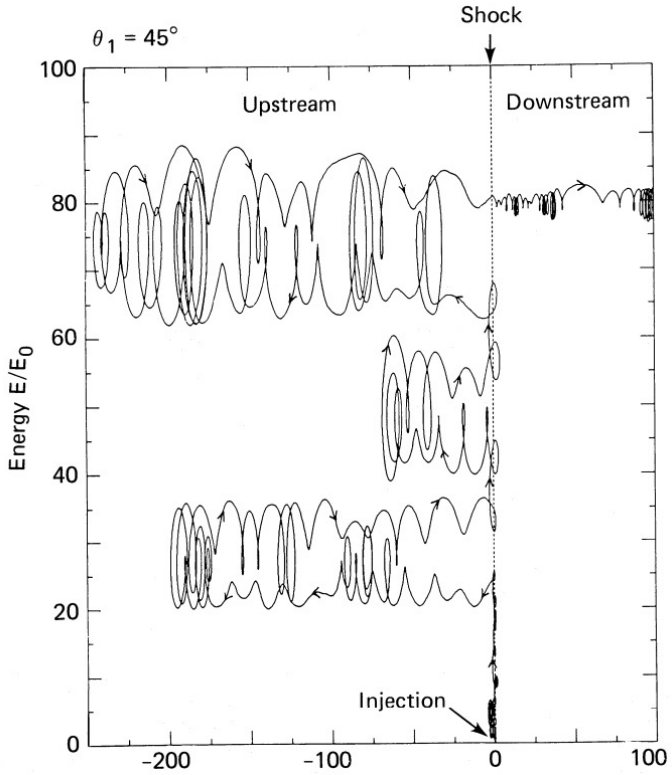

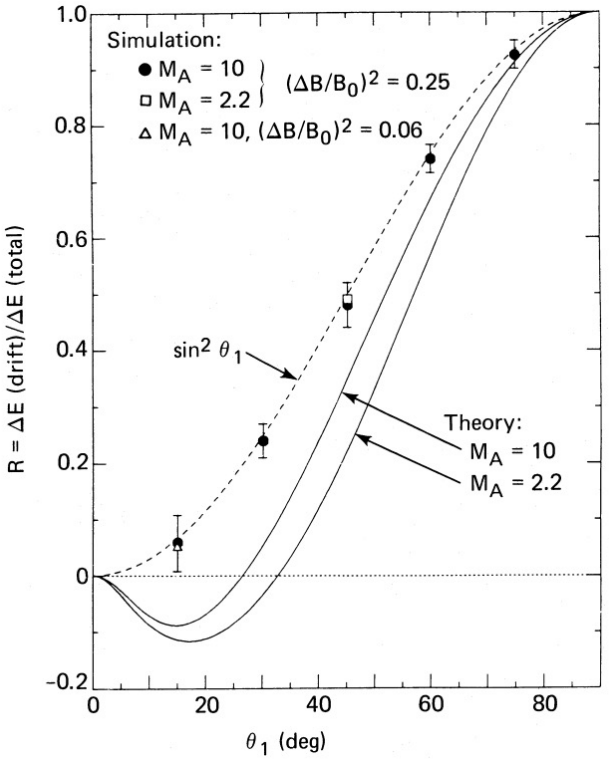

The Electron Injection

electrons with < 0.1-1 MeV cannot be scattered by MHD waves $\omega - kv_{||} = \Omega/\gamma$

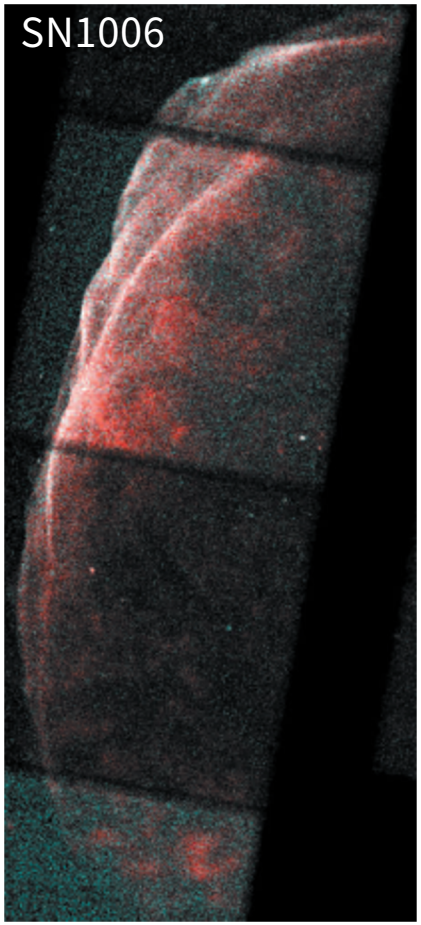

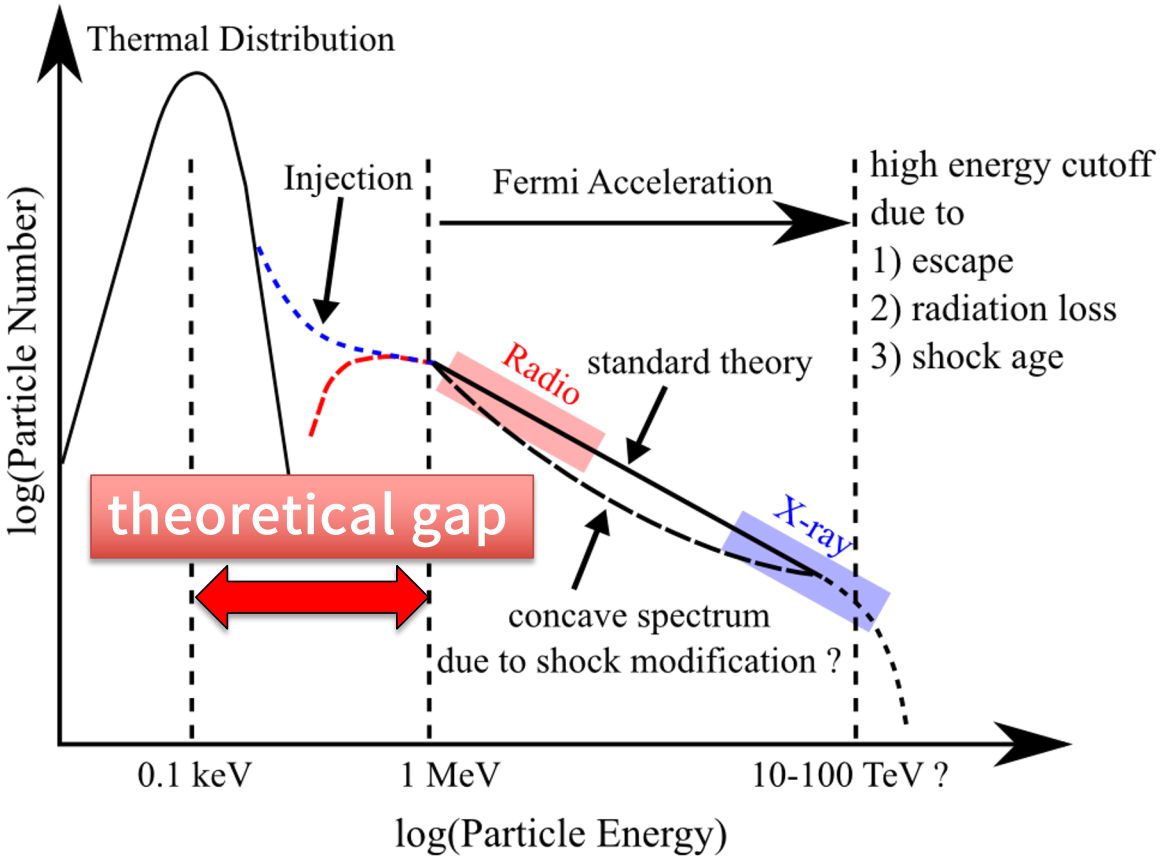

- ✓ Sub-relativistic electrons cannot be accelerated by the standard first-order Fermi mechanism.
- ✓ Substantial energy gain is needed from thermal to relativistic energies by some other mechanisms.
- ✓ Sub-relativistic suprathermal electrons are "invisible" with typical astrophysical observations, while they are observable with in-situ spacecraft measurement.

Ref: Levinson 1992, Amano & Hoshino 2010, Shimada+1999, Lario+2003, Dresing+2016

Acceleration Time and Injection Problem

$$\tau_{acc}(p) = \int_{p_0}^{p} \frac{dp'}{p'} \frac{3}{V_1 - V_2} \left[\frac{\kappa_1}{V_1} + \frac{\kappa_2}{V_2} \right] \sim \frac{\kappa}{V^2} \propto \left(\frac{v}{V} \right)^2 \frac{1}{D_{\mu\mu}}$$

Quasi-linear estimate: $D_{\mu\mu} = \frac{\pi}{4} \frac{k_{\rm R} P(k_{\rm R})}{B_0^2} \Omega_0 \quad \text{where} \quad k_{\rm R} = \Omega_0 / v\mu$

The gyroradii of low-energy electrons are very small and will be well below the dissipation range of MHD turbulence.

→ no electron acceleration should be expected?

- MHD waves cannot resonantly scatter sub-relativistic electrons.
- Intense high-frequency (whistler) waves to scatter low-energy electrons?
- Any other mechanisms to energize low-energy electrons to mildly relativistic energies?

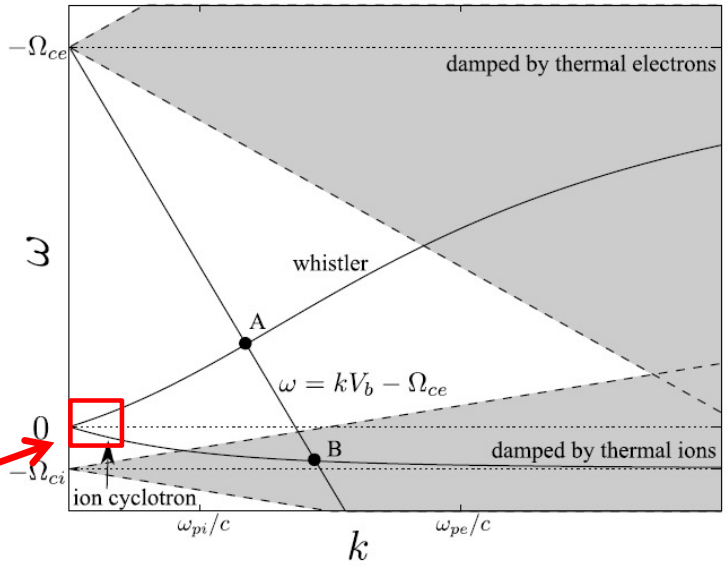

MHD regime
(Alfven waves)

Amano & Hoshino (2010)

Electron Injection Scenario

DSA (diffusion length >> shock thickness)

- Diffusive and slow particle acceleration well beyond the shock thickness.
- The canonical power-law: $f(p) \propto p^{-4}$
- It may operate only when SSDA provides sufficiently energetic electrons.

SSDA (diffusion length ~ shock thickness)

- Diffusive and fast particle acceleration within the shock transition layer.
- It results in a steeper power-law for energy-independent diffusion (consistent with observations at the bow shock.)
- Higher-energy electrons will eventually escape toward upstream because of diffusion lengths longer than the shock thickness.

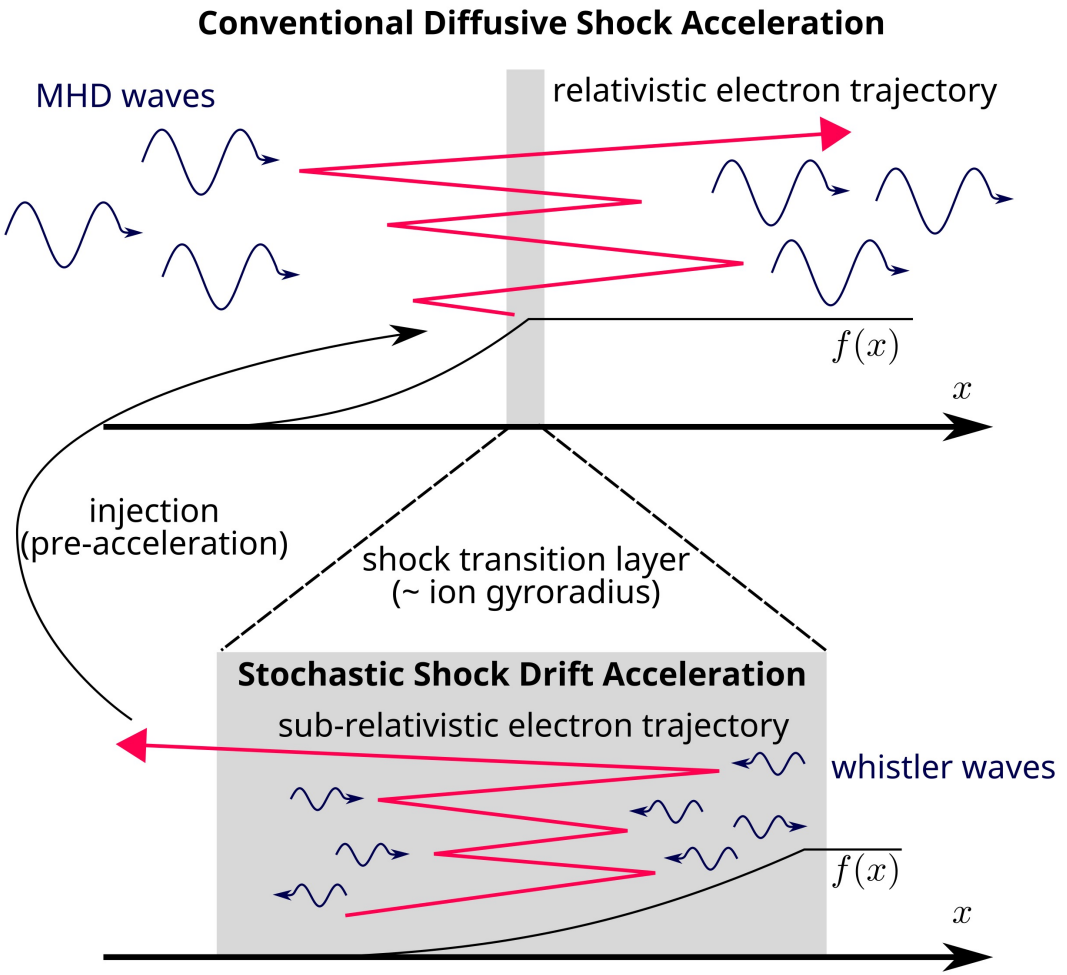

Amano+(2020, PRL), Katou & Amano (2019, ApJ), Kobzar+(2021, ApJ), Matsumoto+(2017, PRL)

Amano & Hoshino (in prep)

Particle Acceleration at Oblique Shock of Finite Thickness

Solutions of the diffusion-convection equation at a shock of finite thickness L_s

$$\frac{\partial f_0}{\partial t} + V\cos\theta\,\frac{\partial f_0}{\partial x} + \frac{1}{3}\left(\frac{\partial \ln B}{\partial x} - \frac{\partial \ln V}{\partial x}\right) V\cos\theta\,\frac{\partial f_0}{\partial \ln p} = \frac{\partial}{\partial x}\left(\kappa\cos^2\theta\,\frac{\partial f_0}{\partial x}\right)$$

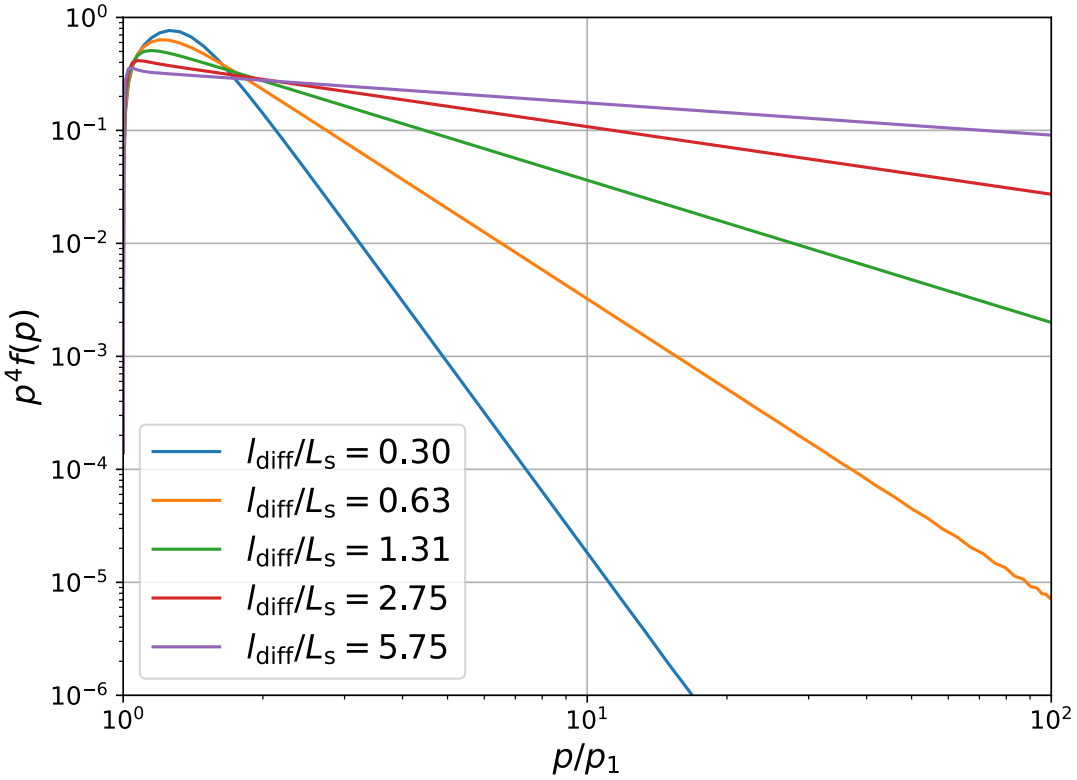

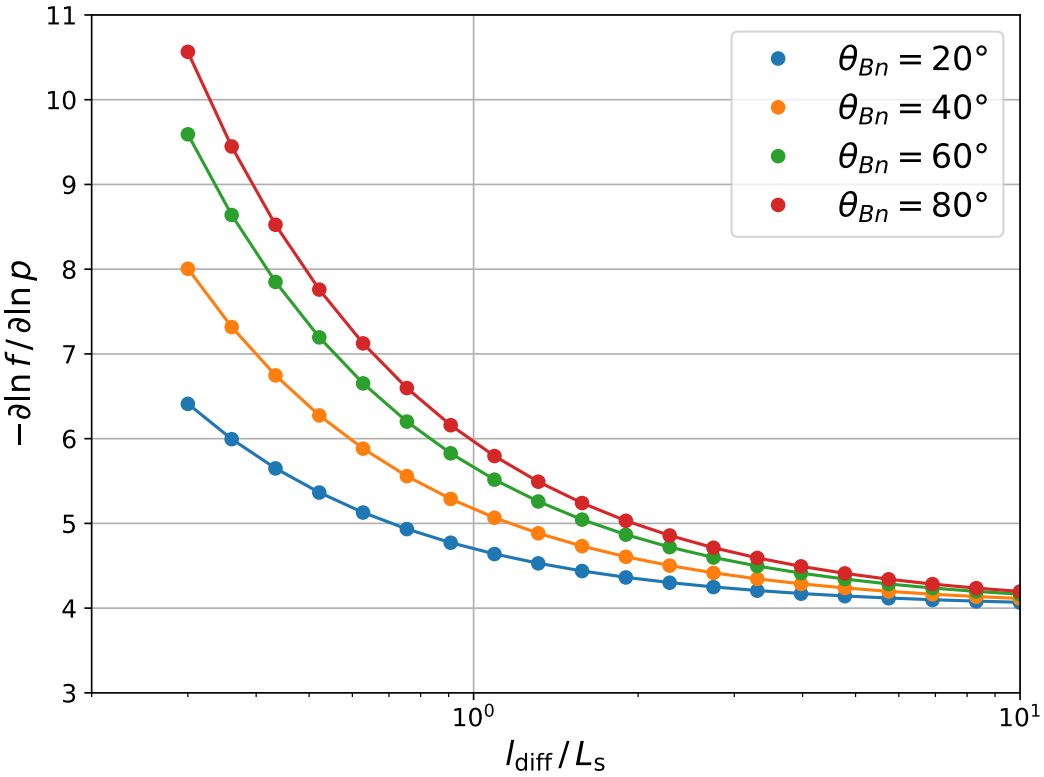

Amano & Hoshino (in prep)

Unifying SSDA and DSA

Both SSDA and DSA may be described by the diffusion-convection equation:

$$\frac{\partial f_0}{\partial t} + V\cos\theta\frac{\partial f_0}{\partial x} + \frac{1}{3}\left(\frac{\partial \ln B}{\partial x} - \frac{\partial \ln V}{\partial x}\right) V\cos\theta \frac{\partial f_0}{\partial \ln p} = \frac{\partial}{\partial x}\left(\kappa\cos^2\theta\frac{\partial f_0}{\partial x}\right)$$

energy gain = flow divergence diffusion along B

$$\frac{\partial}{\partial x}(V\cos\theta) = -V\cos\theta\left(\frac{\partial \ln B}{\partial x} - \frac{\partial \ln V}{\partial x}\right),$$

Both SDA (∇B) and first-order Fermi (∇V) contributes to the energy gain but ∇B is dominant at quasi-perp shocks

The steady-state spectrum may be estimated as $f_2(p) \propto p^{-q}$ with

diffusion length >> shock thickness
→ standard DSA (q=4)

$$q = \frac{3V_1\cos\theta_1}{V_2\cos\theta_2 - V_1\cos\theta_1} = \frac{3r}{r-1},$$

diffusion length ~ shock thickness
→ SSDA

$$q \approx 3\left[1 + \left(l_{\rm diff}\left\langle\frac{\partial \ln B}{\partial x}\right\rangle\right)^{-1}\right],$$

ratio between diffusion length and shock thickness
→ predicted spectrum is steeper than DSA (q>6), but the acceleration time is much shorter

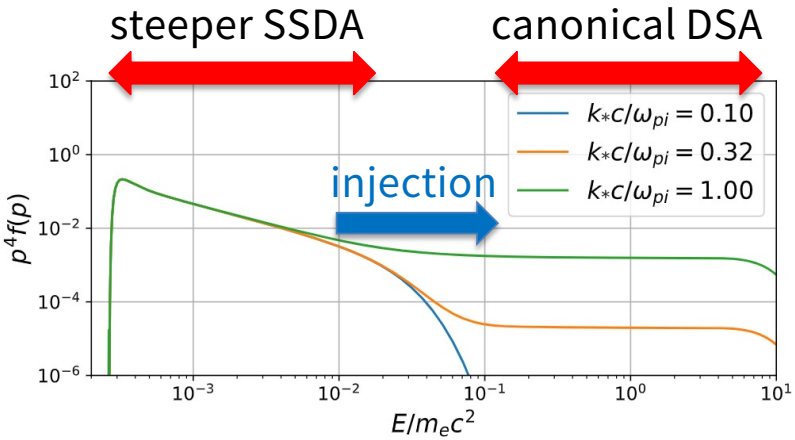

downstream spectrum

Amano & Hoshino (in prep)

- A steep spectrum at low energy and the harder DSA spectrum at high energy may be connected smoothly, if parameters chosen appropriately.
- This indicates that the electron injection and further acceleration to ultra-relativistic energy may be described by a single model.
- The question is what is the condition for injection.

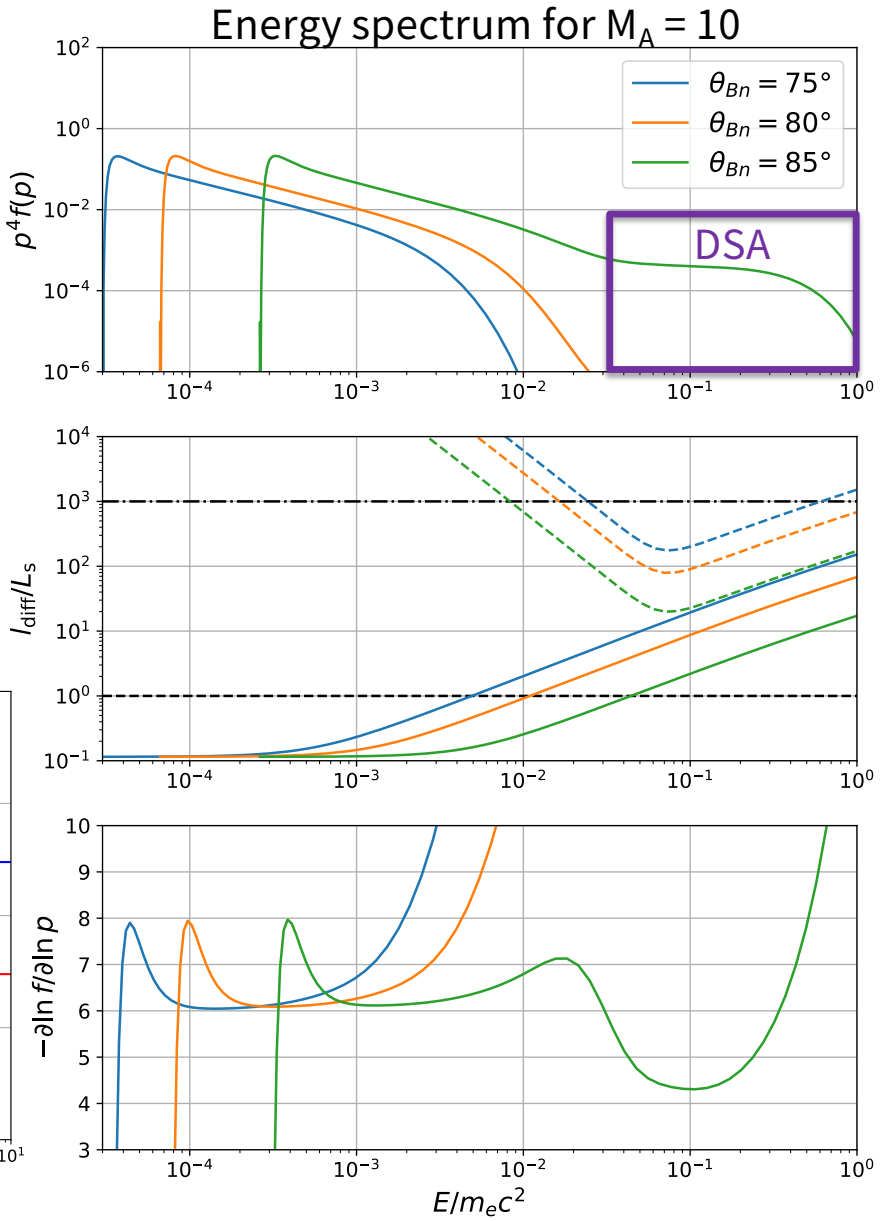

observation

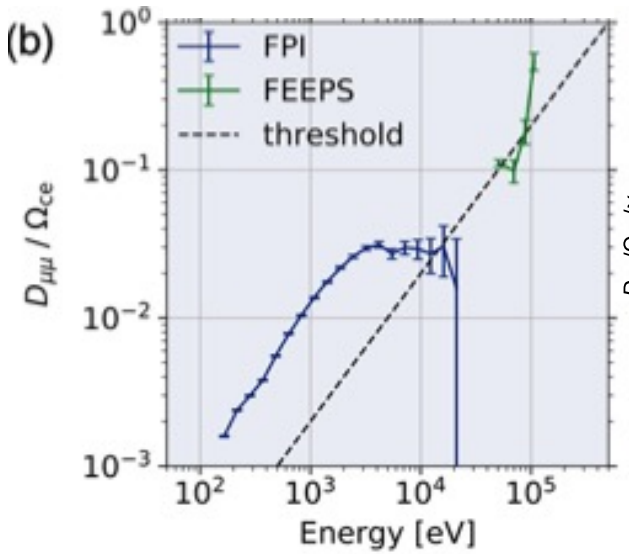

model

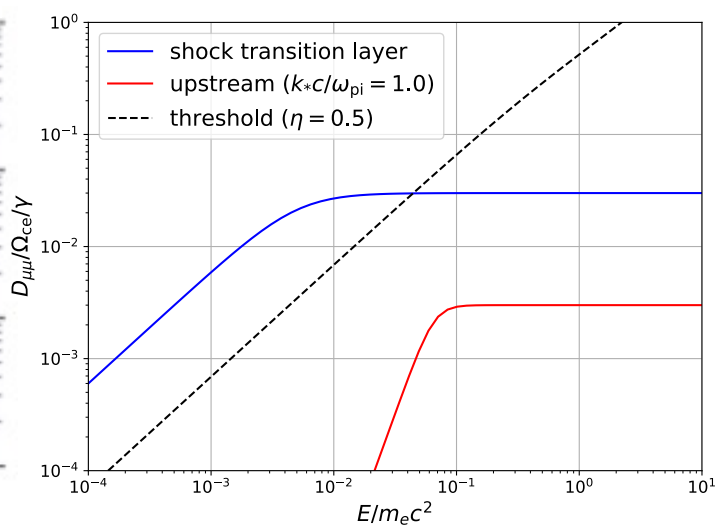

Earth's Bow Shock: Laboratory for Electron Injection

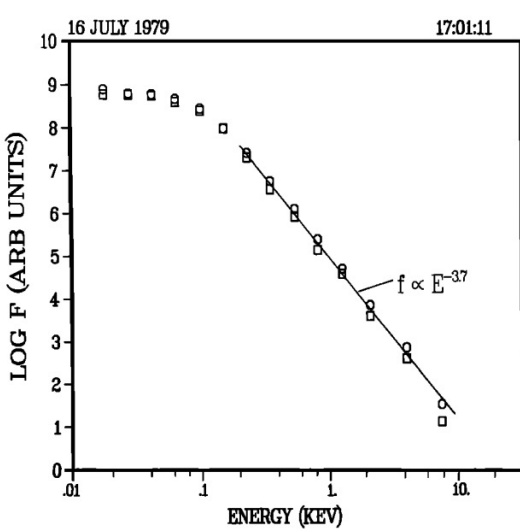

Gosling+1989

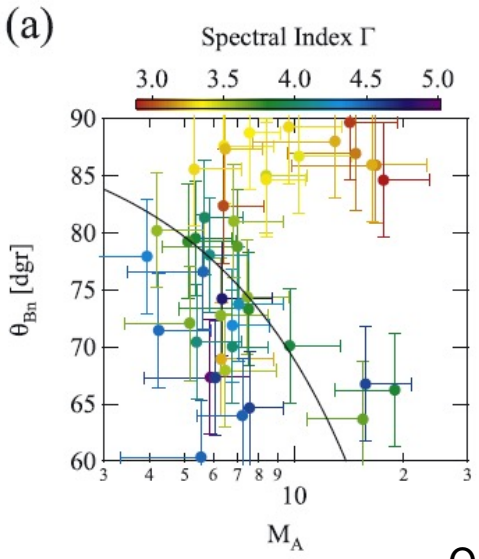

Oka+2006

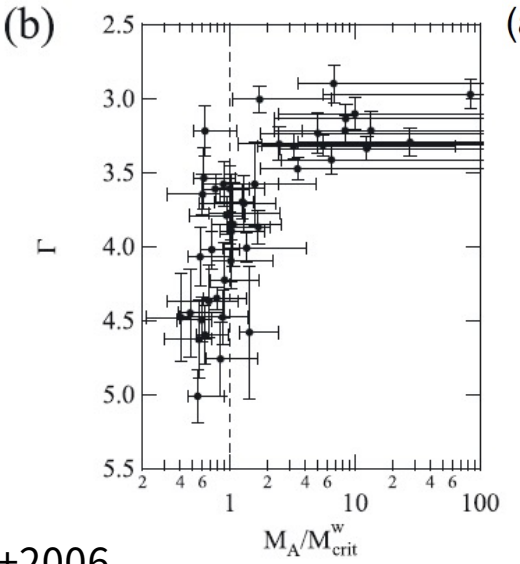

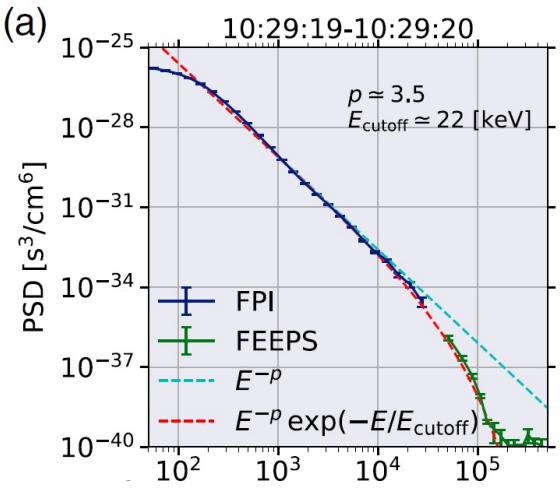

Amano+2020

- Non-thermal electrons with a clear power-law spectrum have been observed occasionally at the bow shock.
- The typical energy range of non-thermal electrons measured at the bow shock is the most important energy range for the injection.

Stochastic SDA (SSDA)

The transport of electrons in the de Hoffmann-Teller frame ($\boldsymbol{u} = u_{\parallel}\boldsymbol{b}$) may be governed by

$$\frac{\partial}{\partial t}f + (v\mu + u_{\parallel})\frac{\partial}{\partial s}f + \left(\frac{1-\mu^2}{2}u_{\parallel}\frac{\partial \ln B}{\partial s} - \mu^2\frac{\partial u_{\parallel}}{\partial s}\right) v\frac{\partial f}{\partial v} - \frac{1-\mu^2}{2}\left((v\mu + u_{\parallel})\frac{\partial \ln B}{\partial s} + 2\mu\frac{\partial u_{\parallel}}{\partial s}\right)\frac{\partial f}{\partial \mu} = \frac{\partial}{\partial \mu}\left[(1-\mu^2)D_{\mu\mu}\frac{\partial}{\partial \mu}f\right] + Q.$$

negligible at Qperp shock (major term for DSA)

mirror force

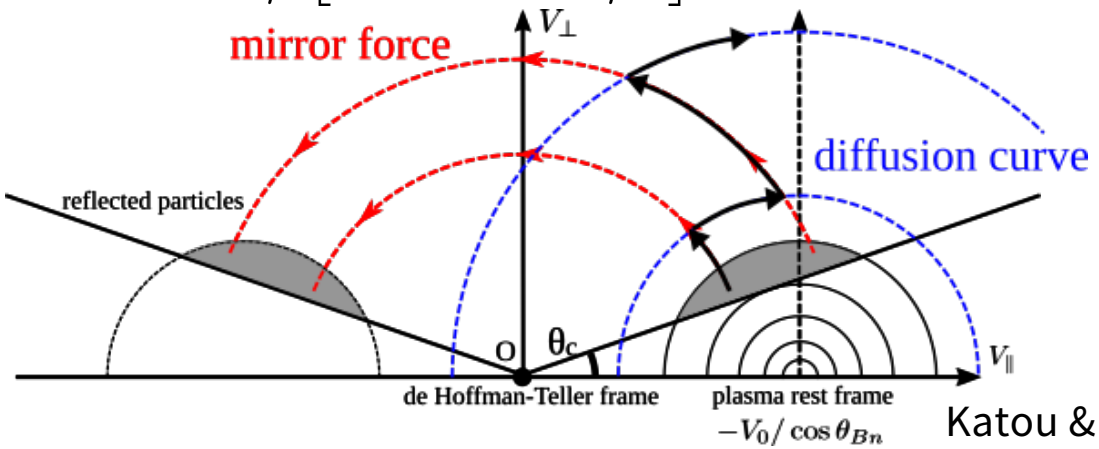

Katou & Amano (2019)

SSDA Signatures

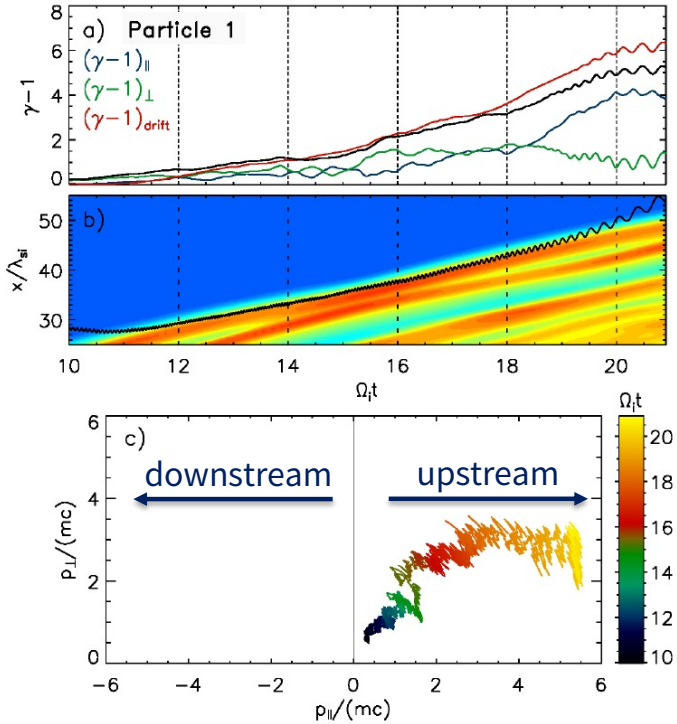

Kobzar+ (ApJ, 2021)
2D high-beta and low Mach no. shock

B field

particle flux

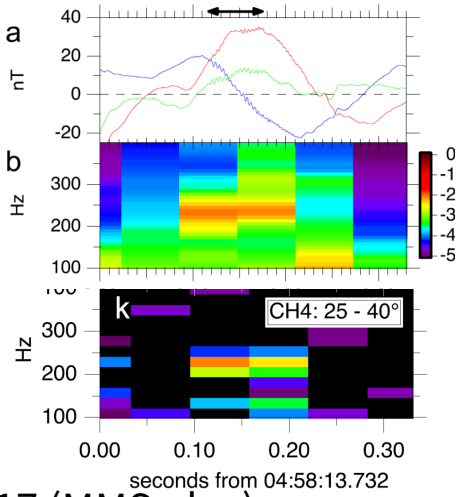

Oka+2017 (MMS obs.)

Stochastic Shock Drift Acceleration
mirror reflection + scattering

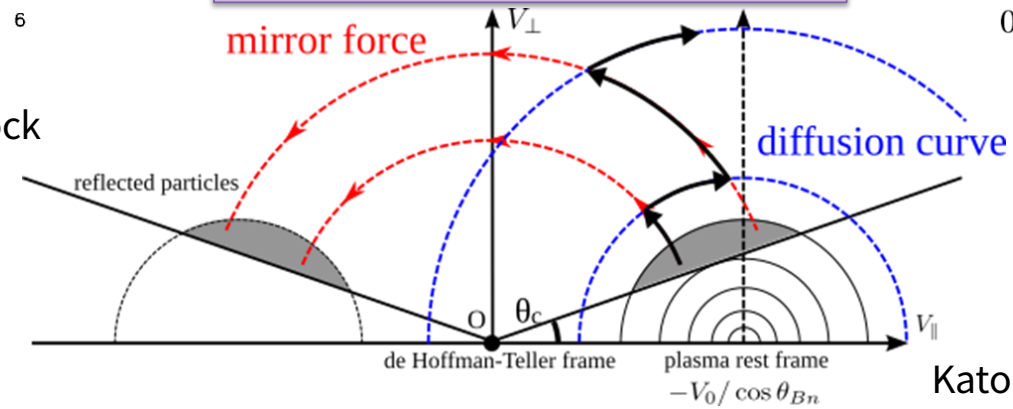

Katou & Amano 2019

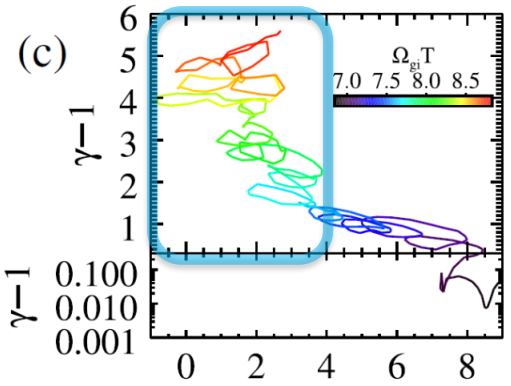

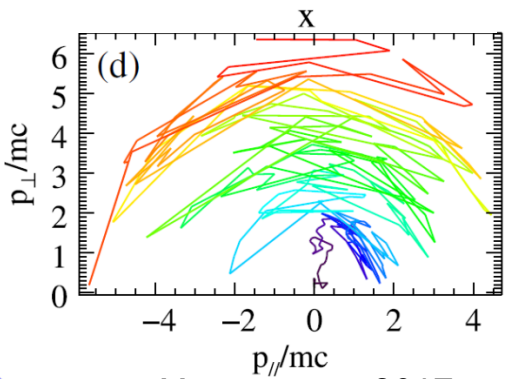

Matsumoto+2017
3D Weibel-dominated shock

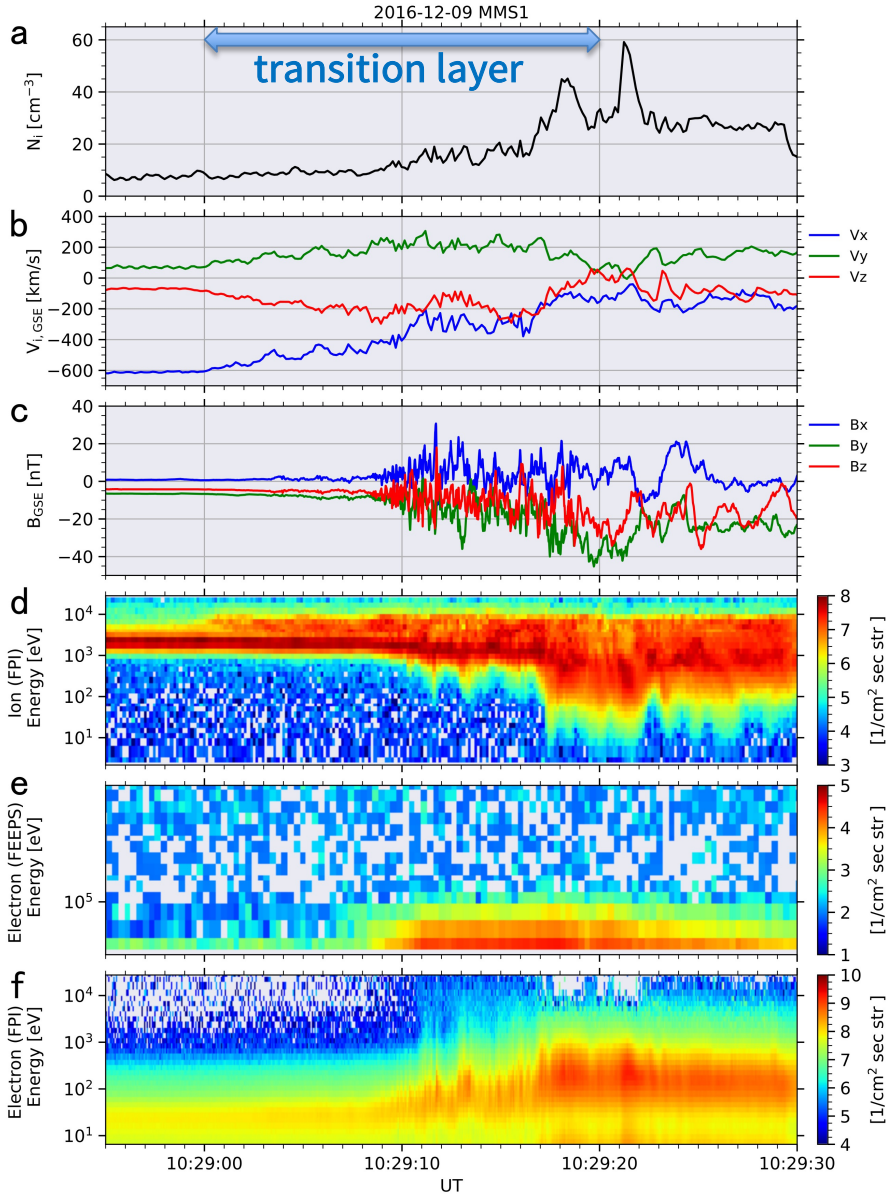

Bow Shock Crossing on 2016 Dec 9

- Vsw ~ 600 km/s
- θ_{Bn} ~ 85 (quasi-perp.)
- M_A ~ 8.9 (high Mach num.)

Substantial flux enhancements for high energy (>1 keV) electrons. FEEPS also detected electrons up to ~100 keV.
Unusual for bow shock crossings.

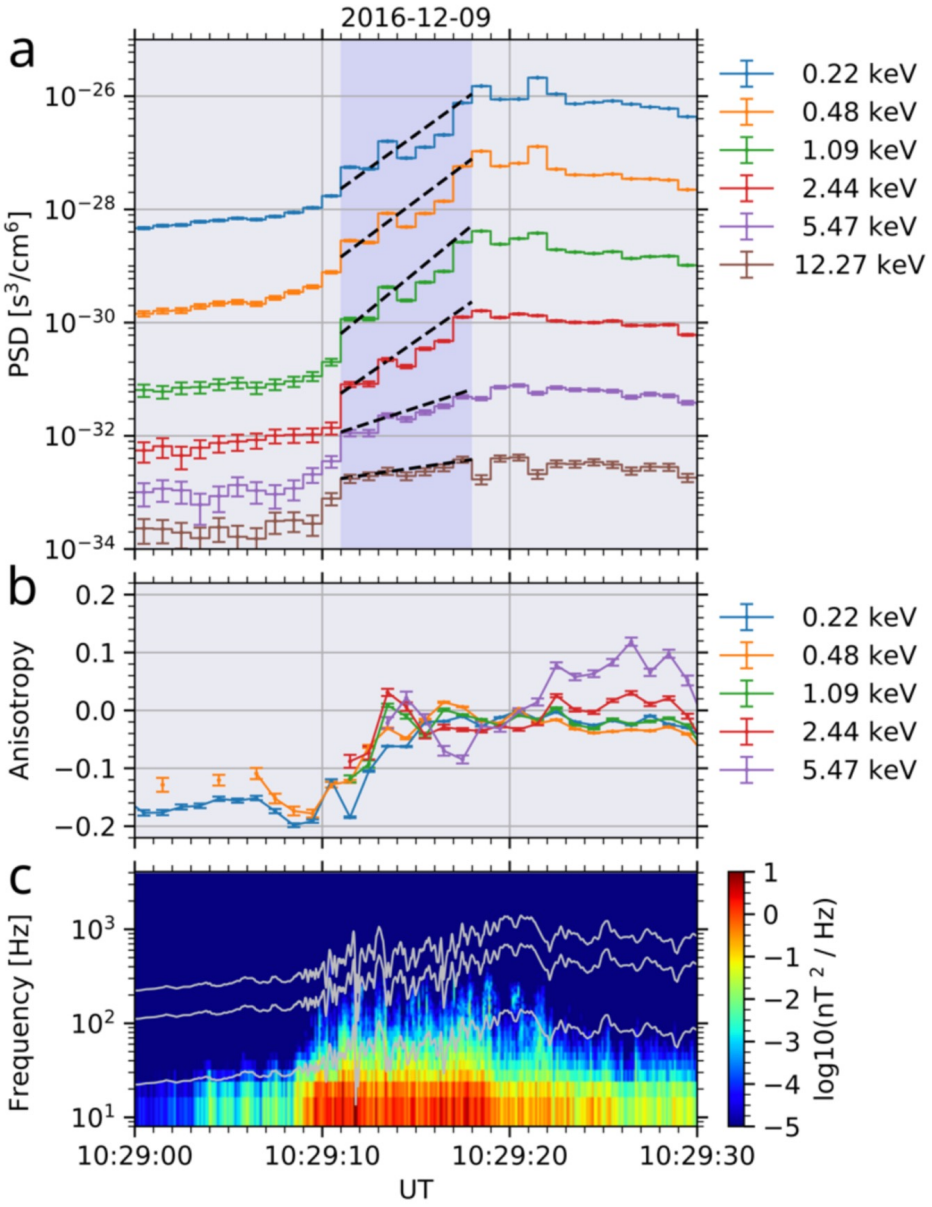

Exponential increase of particle intensity

Nearly isotropic pitch-angle distribution

Enhanced wave power (in particular, high-frequency whistlers)

Smoking-Gun Evidence ?

- Simultaneous appearance of energetic electron profiles, weak anisotropy, enhanced wave power are all consistent with the theory. However, the agreement is only qualitative.
- The observed power-law index is roughly consistent with the theory. But it does not necessarily identify the mechanism.
- The theory predicts that the high-energy cutoff of the spectrum is determined by the single parameter $D_{\mu\mu}$

$$E_{\mathrm{cutoff}} \sim E_{\mathrm{sh}} \left(\frac{m_i}{m_e}\right) \left(\frac{D_{\mu\mu}}{\Omega_{\mathrm{ce}}}\right) = \frac{1}{2} m_i \left(\frac{u_0}{\cos\theta_{\mathrm{Bn}}}\right)^2 \left(\frac{D_{\mu\mu}}{\Omega_{\mathrm{ce}}}\right)$$

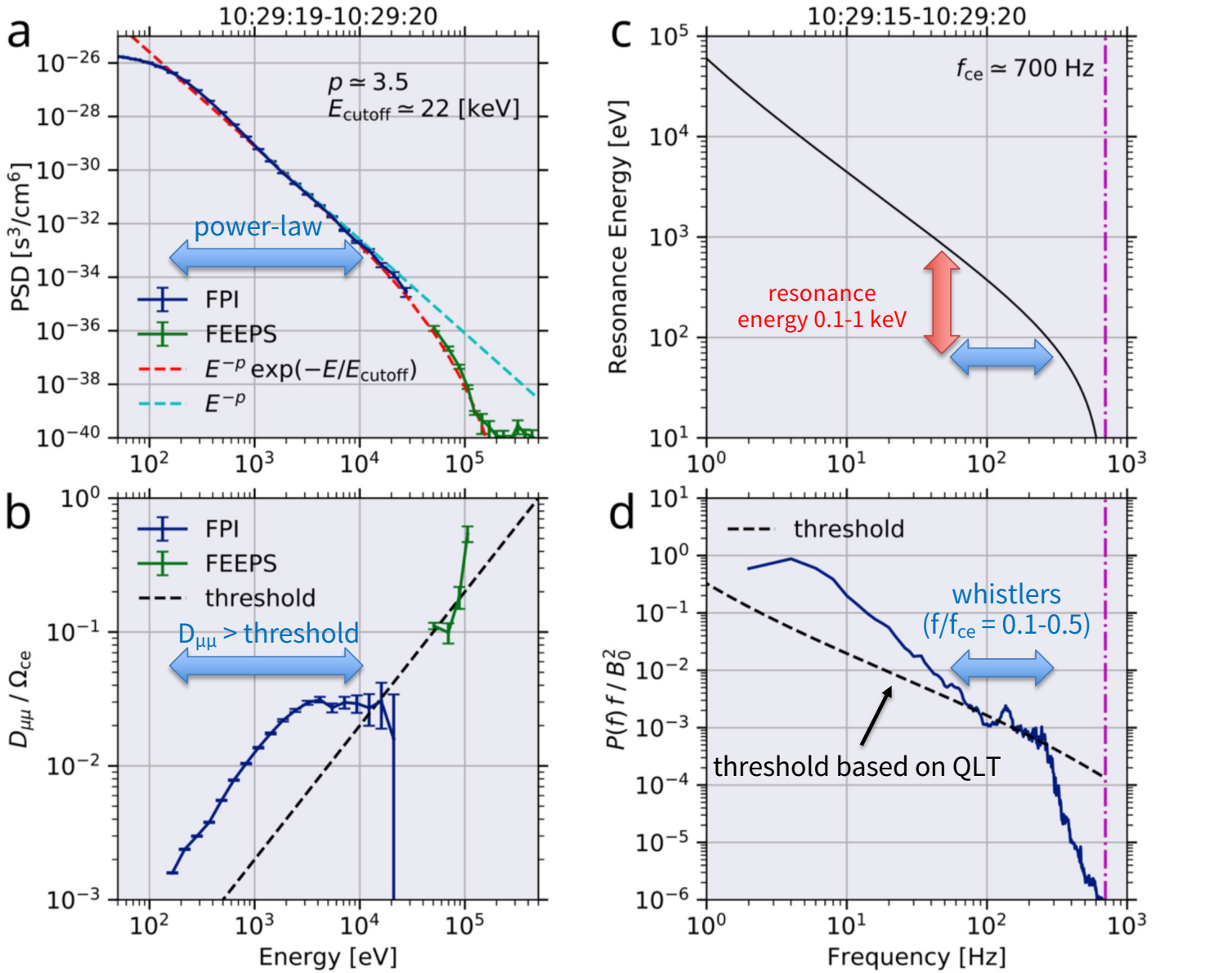

Amano+(2020, PRL)

ここまでのまとめ

- 電子の輸送方程式が拡散で書けるのであれば，上手くパラメータ（拡散係数）を選べば非相対論的エネルギーから相対論的エネルギーまでの電子加速が記述でき，スペクトルも求まる．宇宙線電子の絶対量も原理的には決まる．
- 問題：拡散係数はどのように決定されるのか？

運動量pの電子を加速できる条件 $$M_{\rm A}^{*} \gtrsim (6\eta)^{-1/2} \left(\frac{D_{\mu\mu}(p)}{\Omega_{\rm ce}} \right)^{-1/2} \left(\frac{p}{p_{\rm A,e}} \right)$$

DSAへの電子の注入条件 $$M_{\rm A}^{*} \gtrsim (6\eta)^{-1/2} \left(\frac{D_{\mu\mu}(p)}{\Omega_{\rm ce}} \right)^{-1/2} \left(\frac{m_i}{m_e} \right)^{1/2} \left(\frac{k_* c}{\omega_{\rm pi}} \right)^{-1}$$

$M_{\rm A}^{*} = M_{\rm A} / \cos\theta_{Bn}$：観測(Oka+2006)や理論(Amano & Hoshino 2010, Levinson 1992-1996)で何故かよく出てくるパラメータ

Super-critical Shock

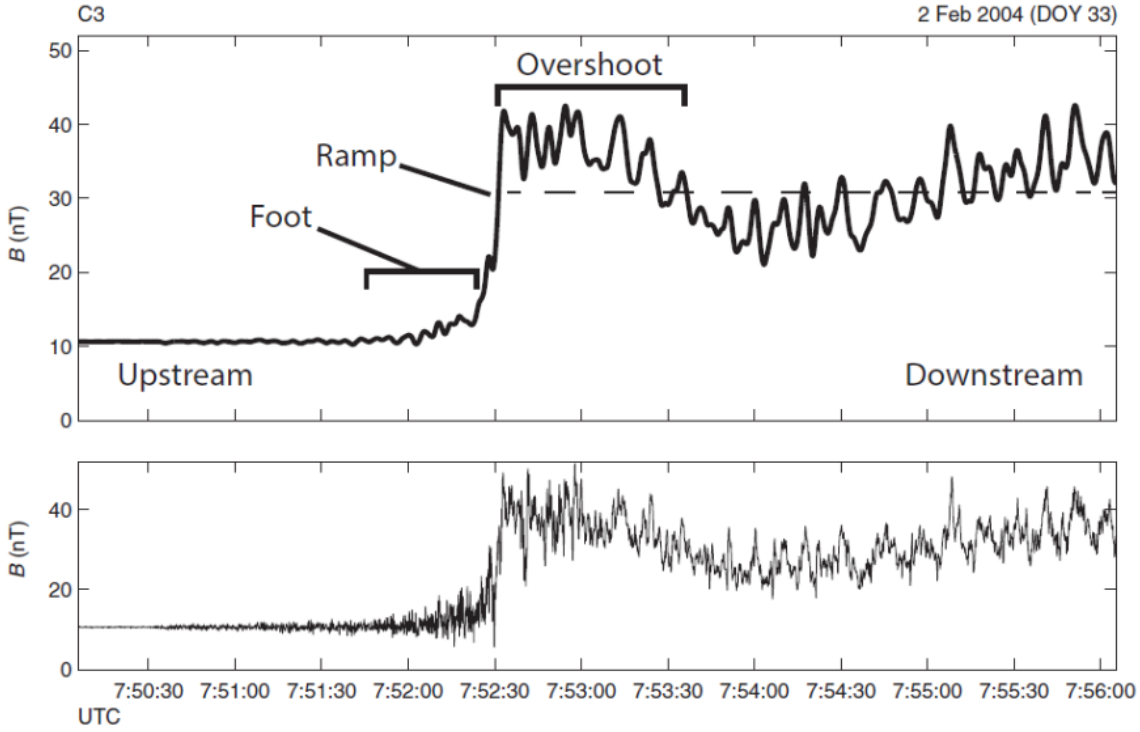

Figure 3.1 Example of a supercritical quasi-perpendicular bow shock crossing as seen in magnetic field magnitude. Lower panel shows high-resolution data at 22 samples per second; upper panel shows data low-pass filtered with a cut-off frequency of 0.2 Hz. A nominal downstream average value is shown with a dashed line. Data from C3 Cluster spacecraft for 2 February, 2004 supplied by Cluster Science Archive. (Plot supplied by T. Sundberg.)

Ion Reflection at Super-critical Shocks

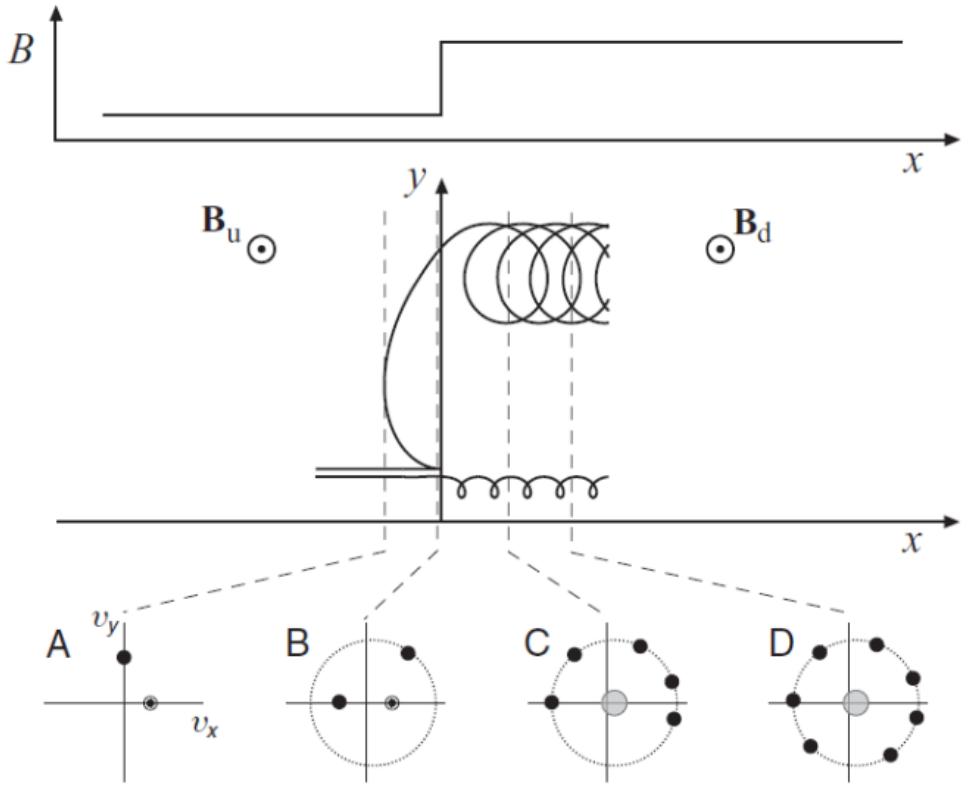

Figure 3.3 Trajectory and velocity space of an ion which is specularly reflected at a perpendicular shock, using a simple model of the reflection process and the shock fields. A trajectory for a transmitted ion is also shown.

Energization of reflected ions by the motional E-field provides the effective "viscous" heating in the sense that the downstream pressure is dominated by the reflected ions.

Johlander+2016, PRL

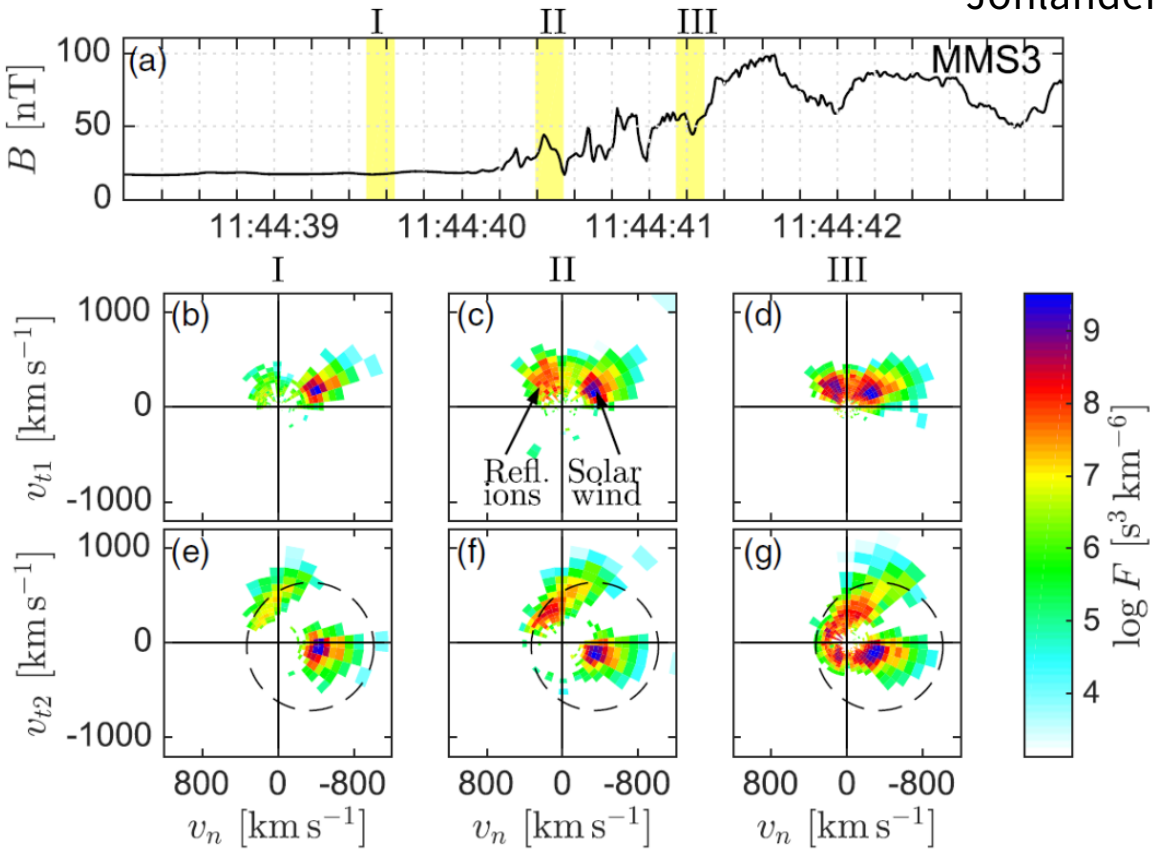

FIG. 2. Snapshots of ion distributions by MMS3. (a) B. (b)–(d) Projected ion phase-space density as a function v_n and v_{t1} at times I–III, (e)–(g) as a function v_n and v_{t1}. The dashed circles indicate which parts of velocity space reflected ions should occupy, assuming specular reflection.

Parallel and Perpendicular Shocks

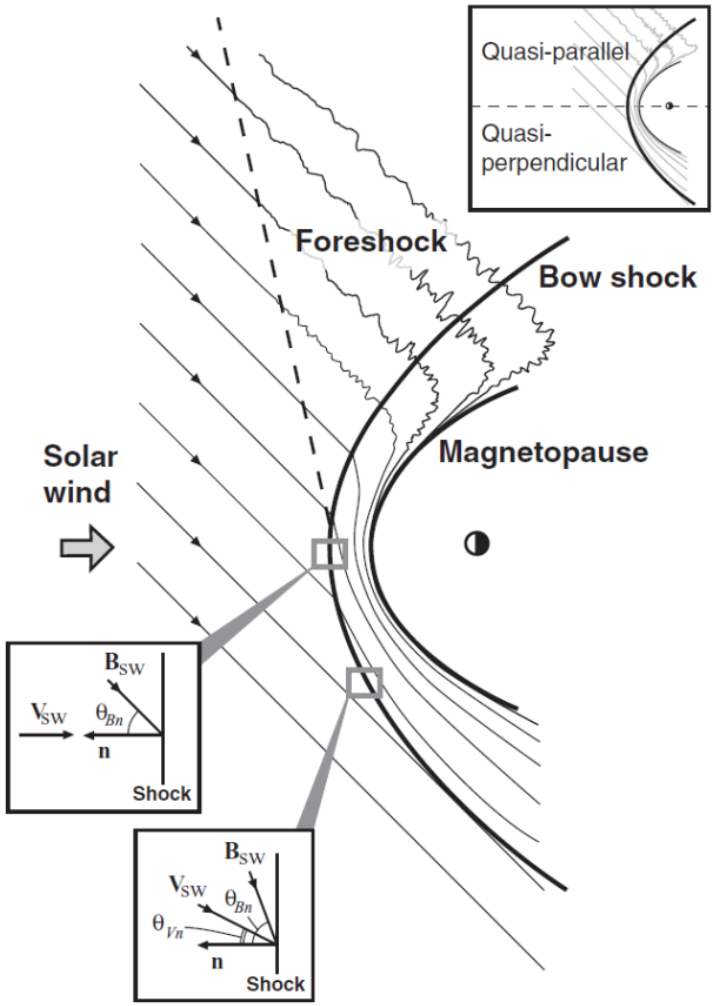

Figure 1.8 The Earth's bow shock system across a plane containing the solar wind flow and interplanetary magnetic field (IMF), with bow shock and magnetopause to scale for average solar wind conditions. The ion foreshock where the upstream field is most strongly disturbed is to the right of the dashed line, indicative of the upstream boundary for shock-accelerated particles. Insets show the shock geometry at the nose and on the flank of the bow shock. Field lines inside the magnetosphere are not shown.

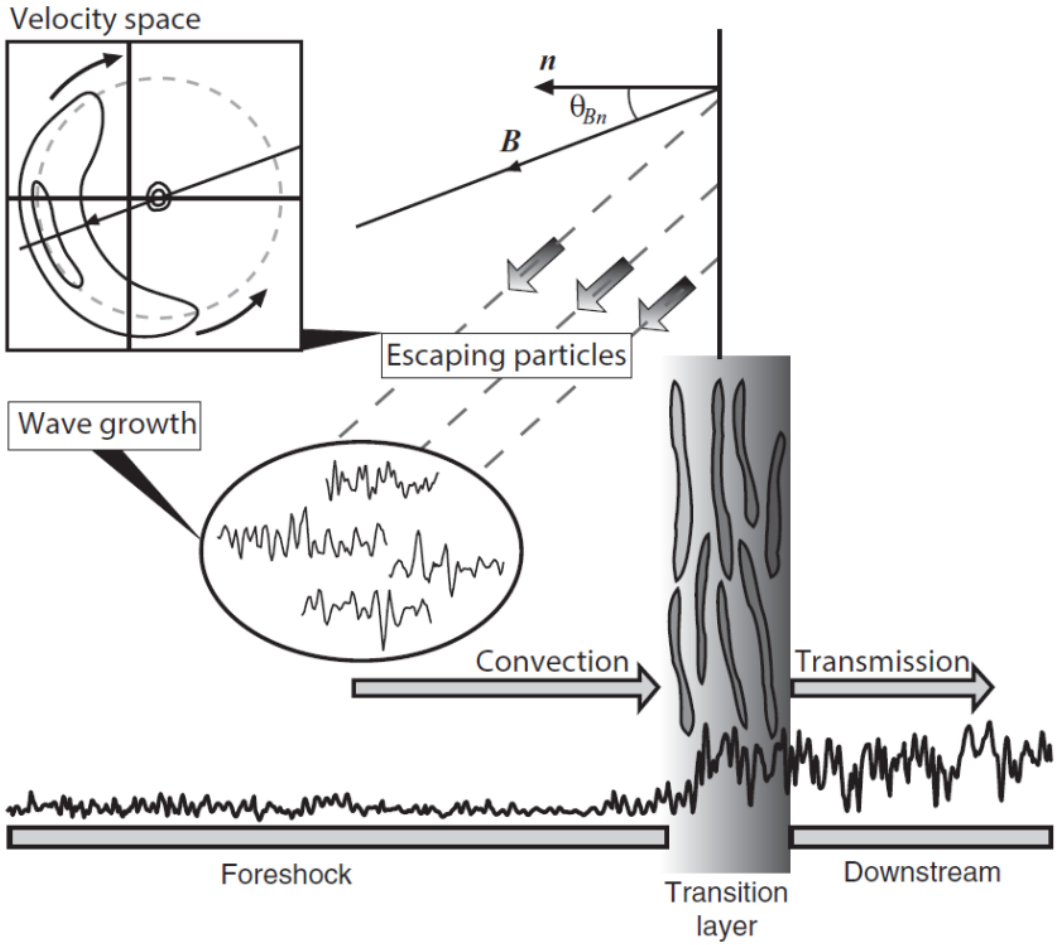

Figure 1.7 Schematic of the various coupled processes operating in the foreshock-shock interaction.

Electron Acceleration Diagram

Saturn's bow shock [e.g., Masters+2013, 2016]

shock surfing (Buneman) + Weibel/Reconnection?
[e.g., Hoshino & Shimada 2002, Matsumoto+2015, 2017, Bohdan+2019]

high M_A

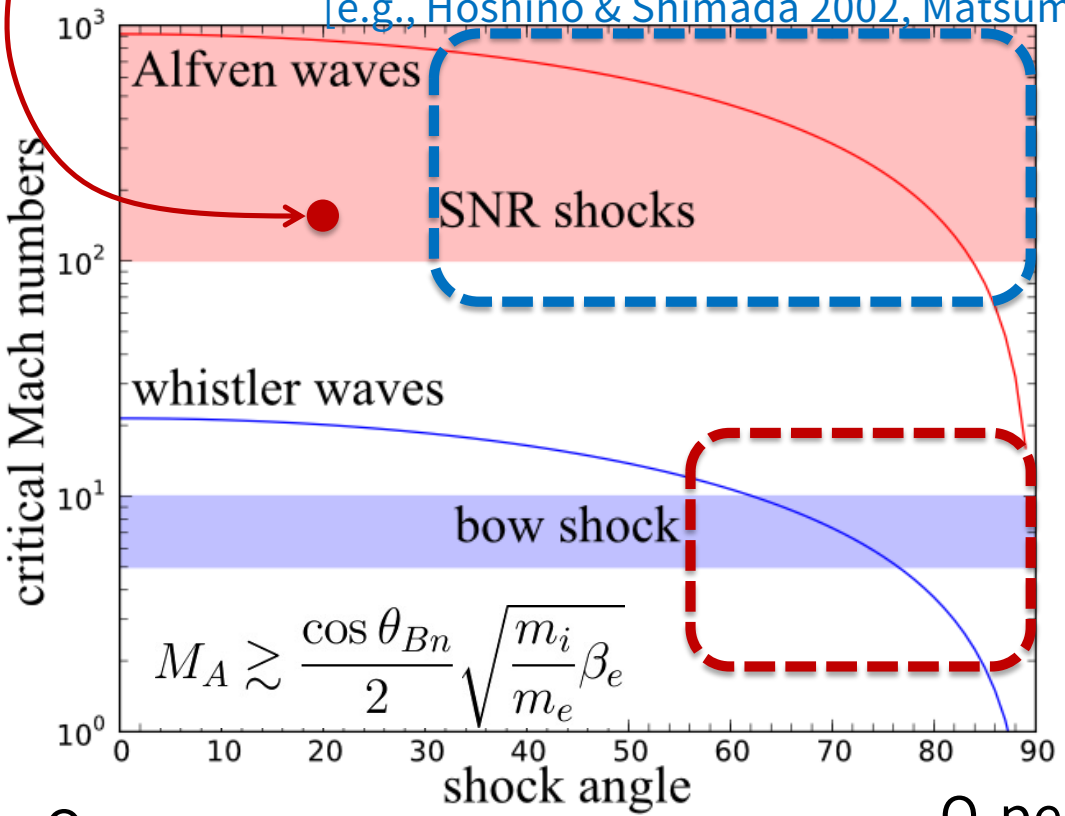

low M_A

Q-para

Q-perp

Earth's bow shock
[e.g., Oka+2006, Amano+2020]

intercluster shocks?

c.f., Amano & Hoshino 2010

Kobzar+2021

Multi-scale Plasma Waves at High-β Shock

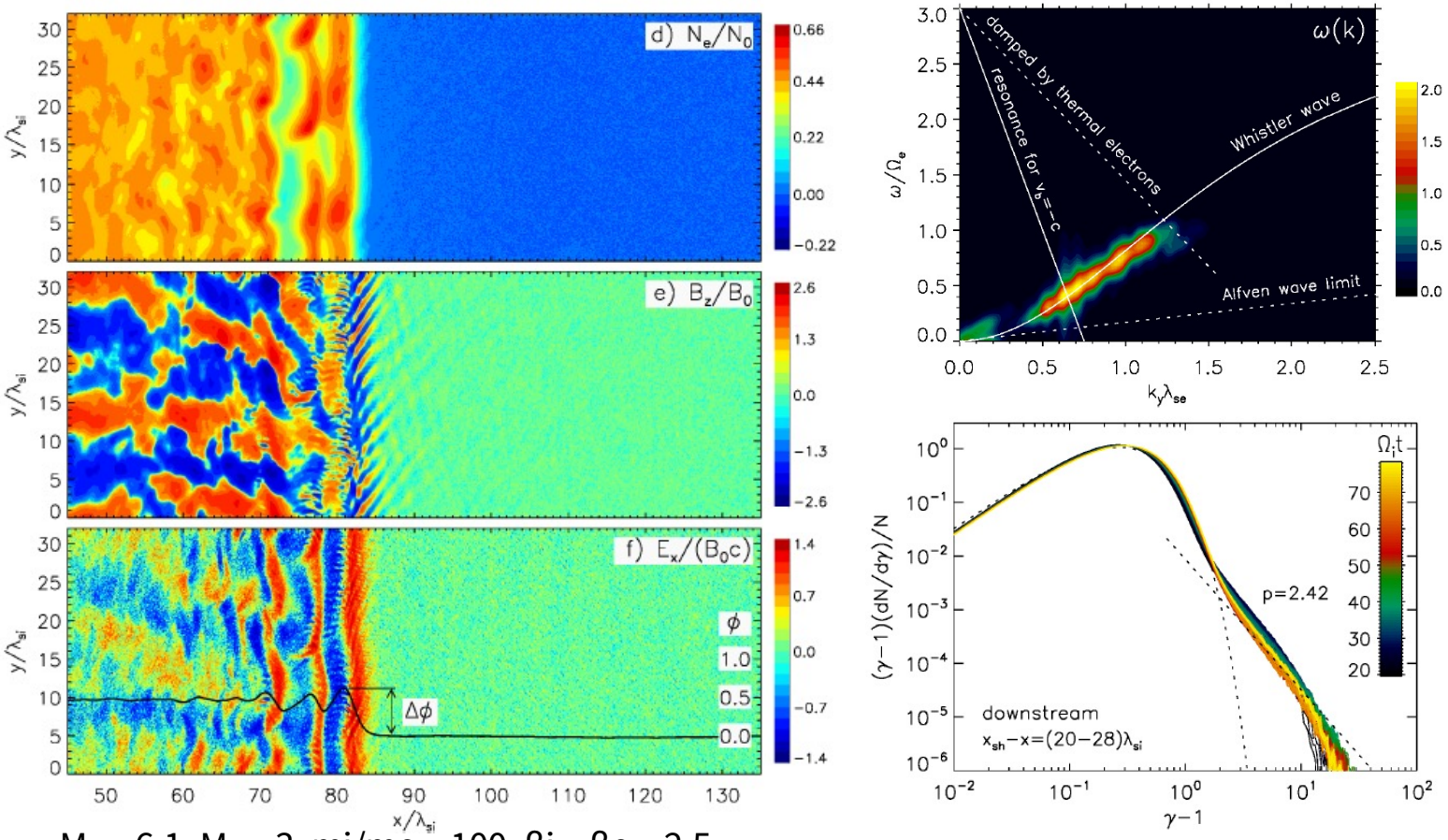

- $M_A = 6.1$, $M_S = 3$, mi/me = 100, βi = βe = 2.5
- Rippling (AIC/Mirror), whistlers, firehose, ES (ion acoustic or Langmuir) waves…
- A clear power-law tail is identified for the downstream spectrum.

Kobzar+2021

SSDA and multiple-SDA

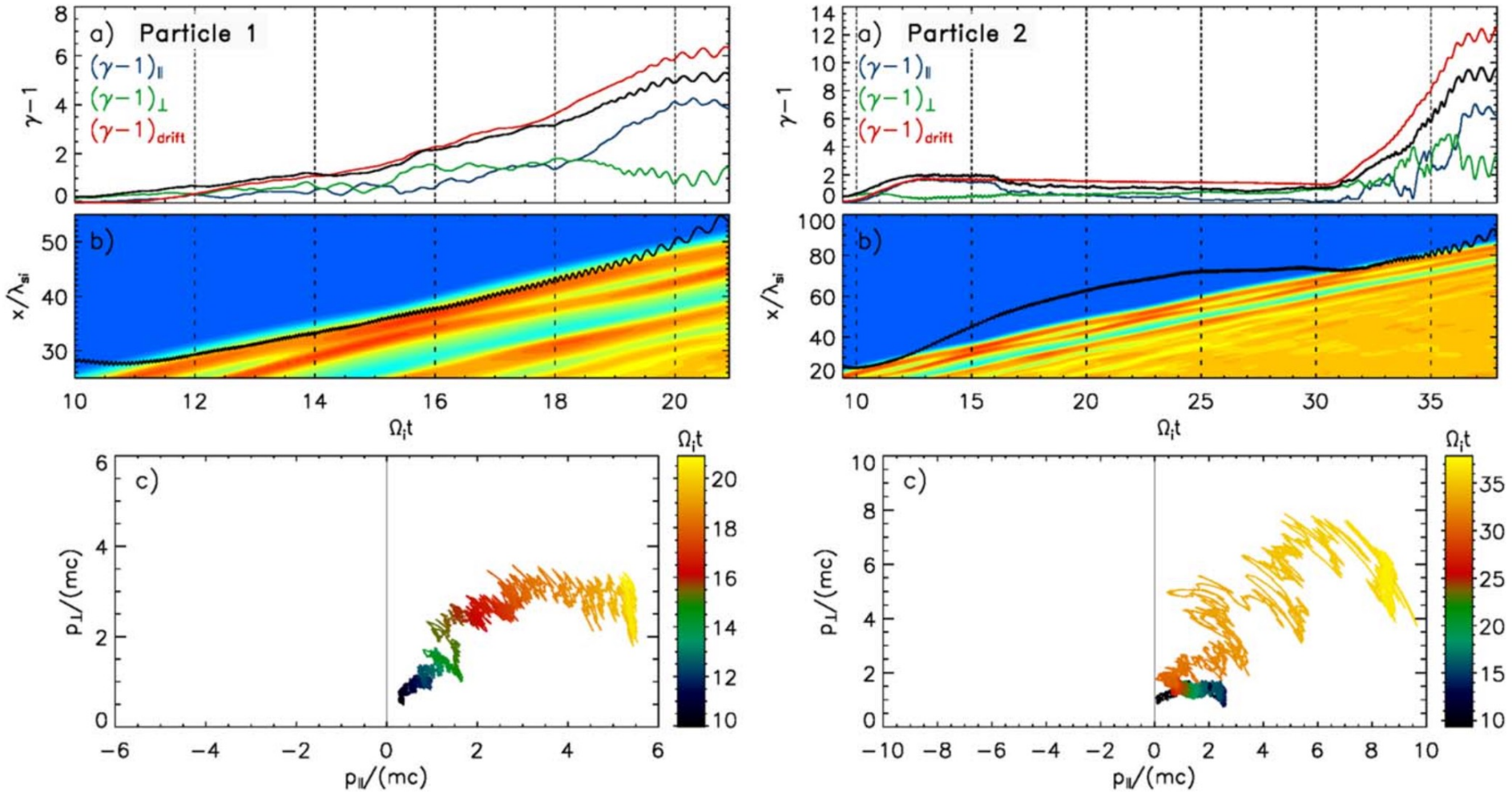

Guo+2014

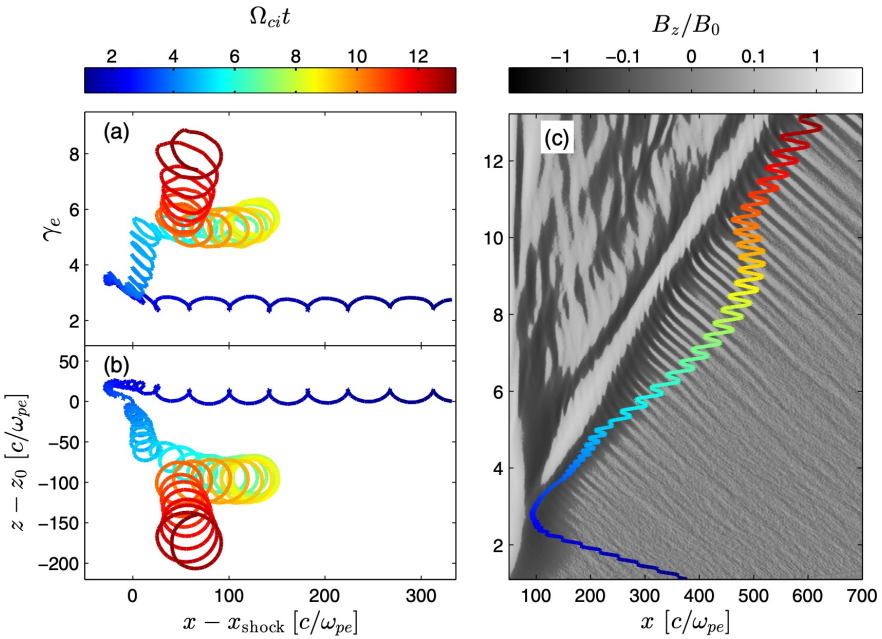

Ha+2021, arXiv:2102.03042

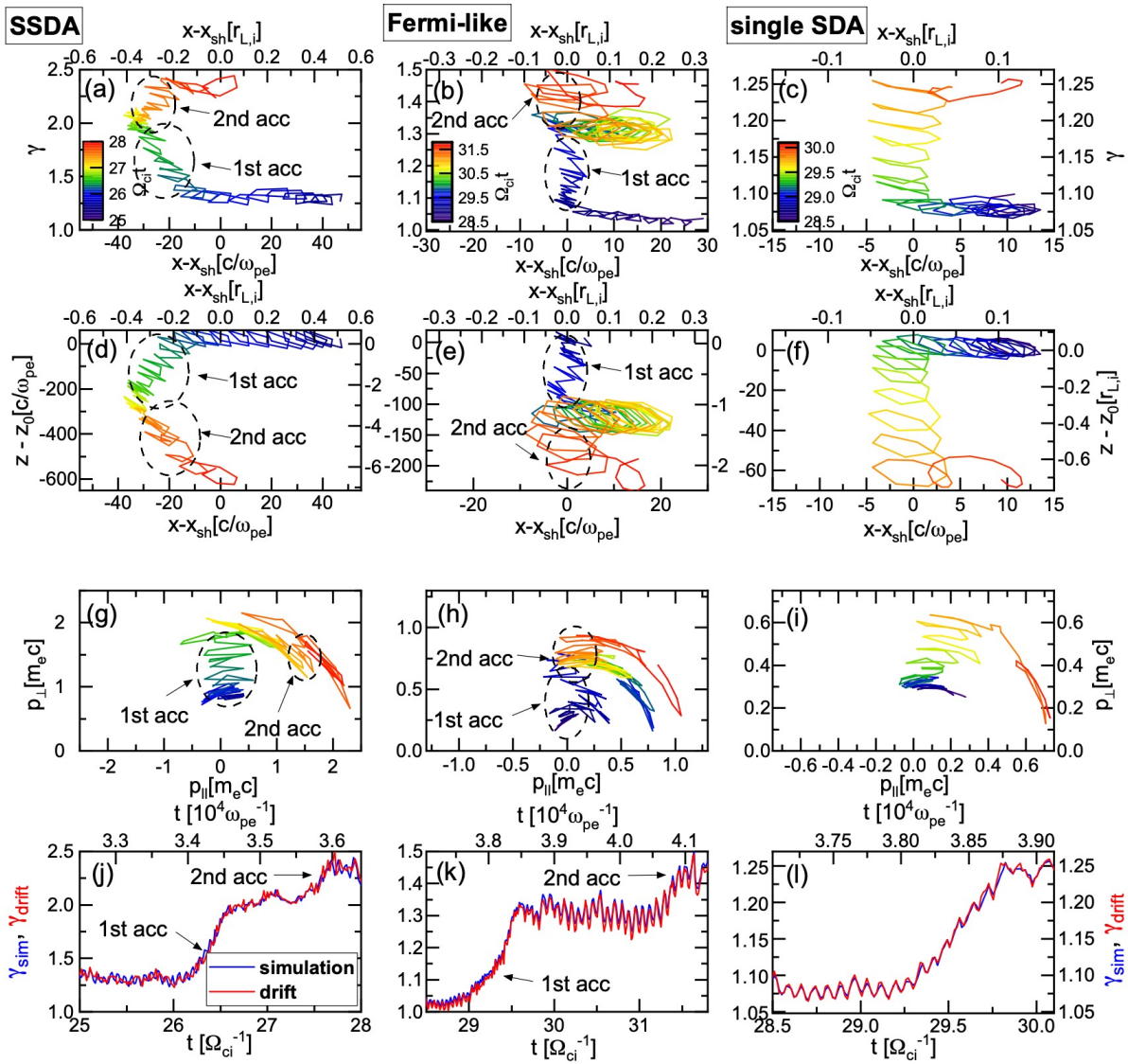

Amano & Hoshino 2007

Injection into SDA/SSDA

SDAには初期にある程度大きなエネルギーを持った電子が必要
→ 別のメカニズムでの加熱・加速

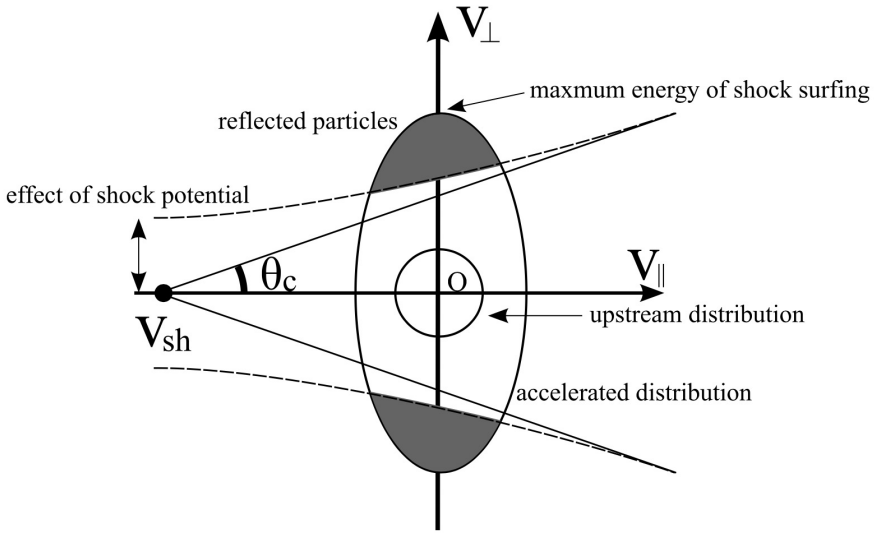

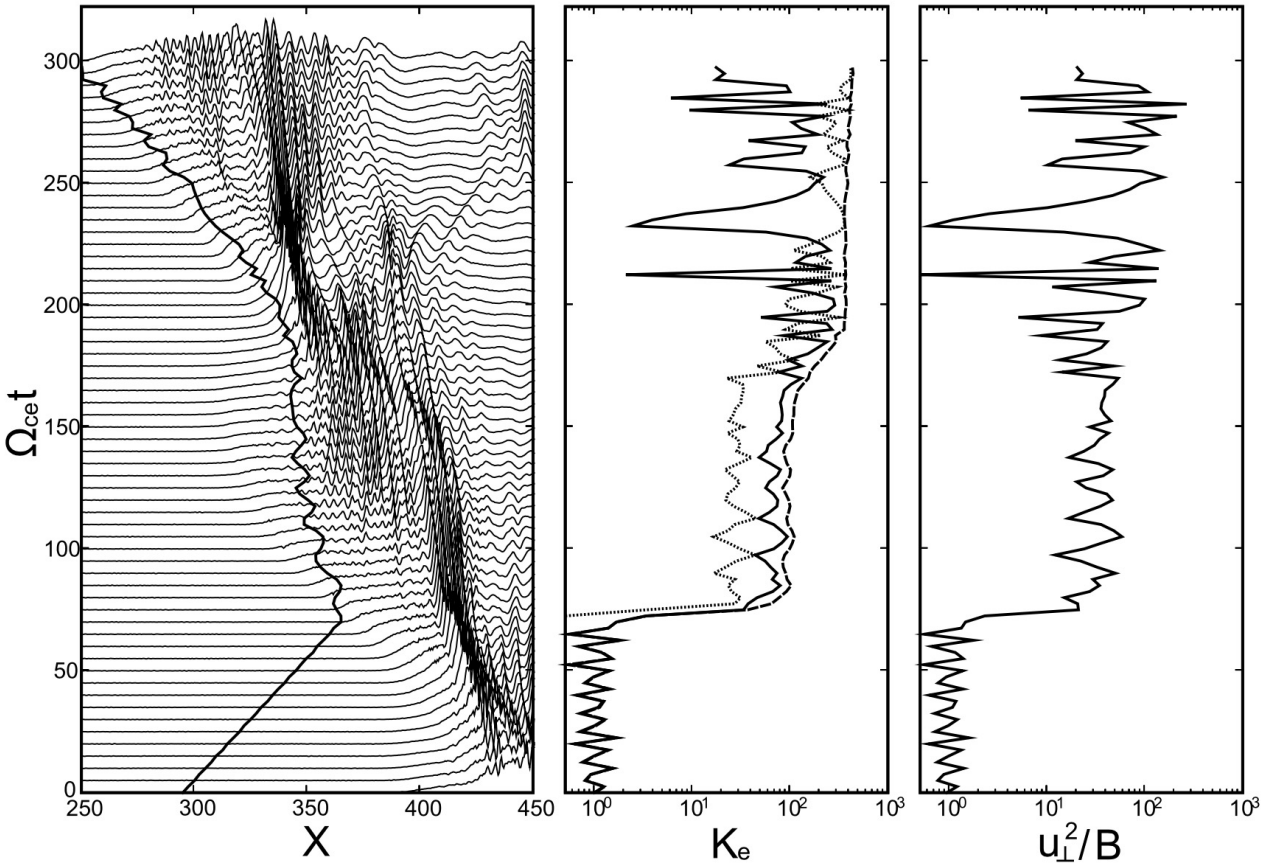

10^{12} particles in
8800 x 768 x 768 cells
($55d_i$ x $4.8d_i$ x $4.8d_i$)

- mi/me=64,
- M_A=20,
- θ_{Bn}=74

3D PIC on the K computer (Matsumoto+2017, PRL)

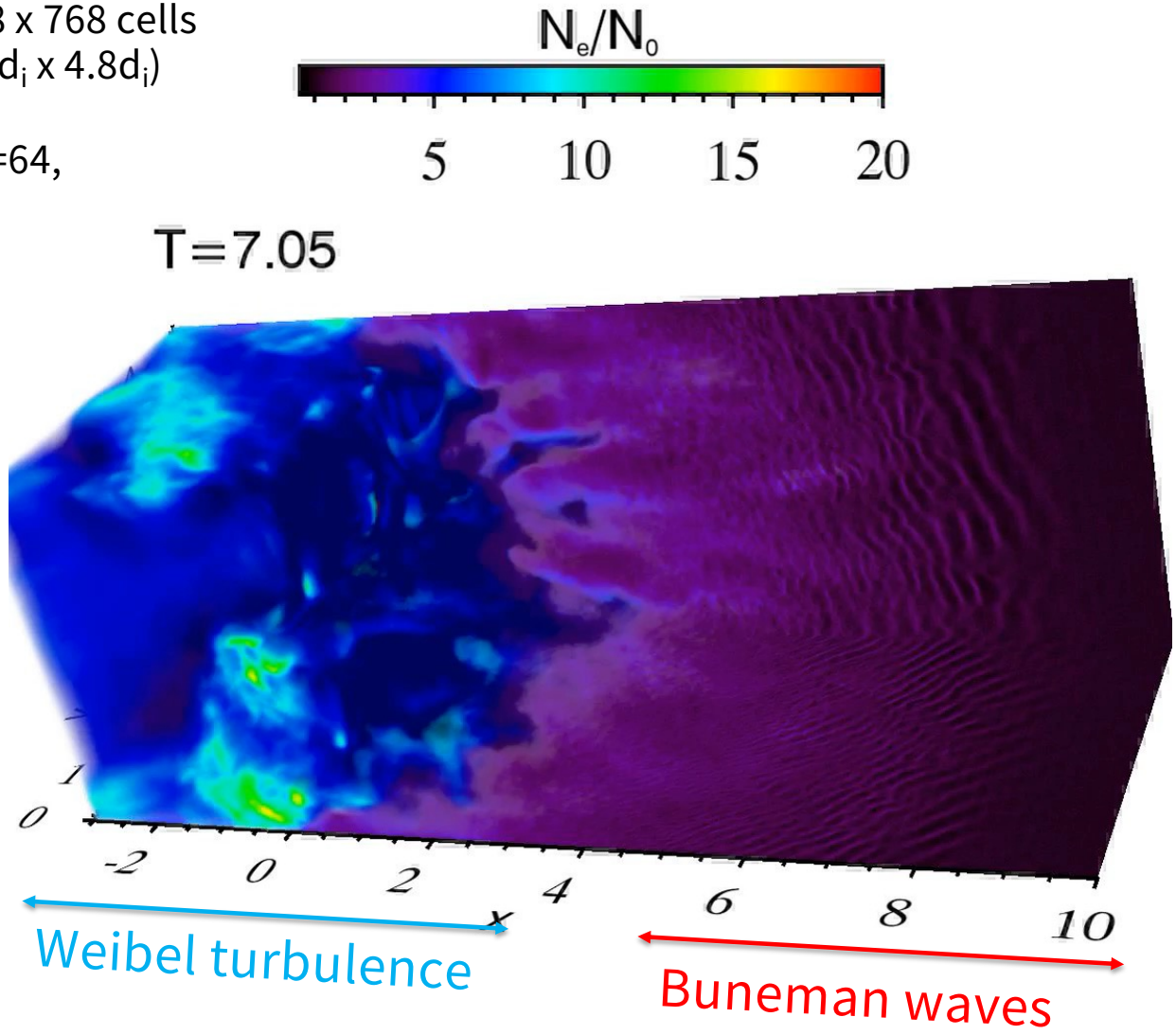

c.f., McClements+2001, Hoshino & Shimada 2002

Shock Surfing Acceleration in 3D

downstream

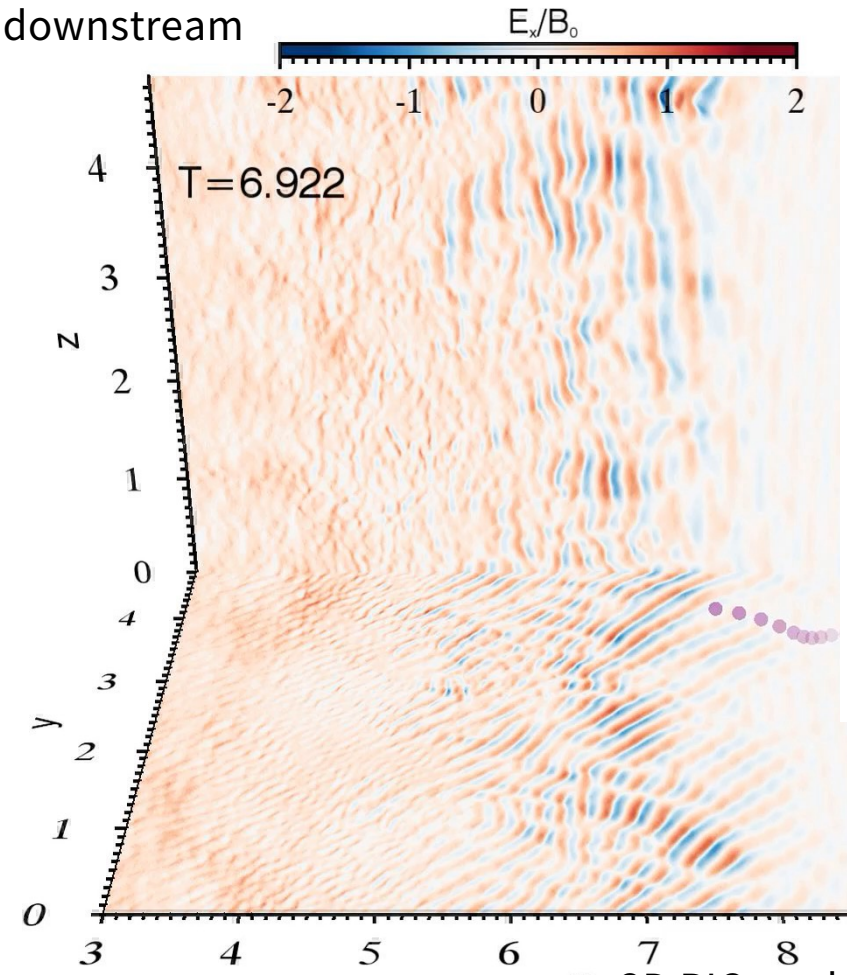

upstream

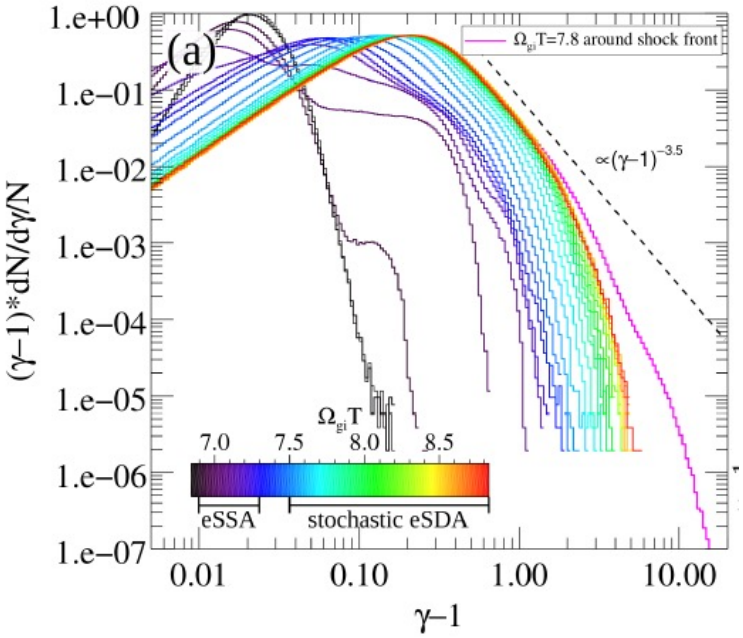

Buneman-generated electrostatic waves in fully 3D
(mi/me = 64, theta = 74, Ma=20)

× 3D PIC on the K computer (Matsumoto+2017, PRL)

3D PIC on the K computer (Matsumoto+2017, PRL)

Shock Drift Acceleration

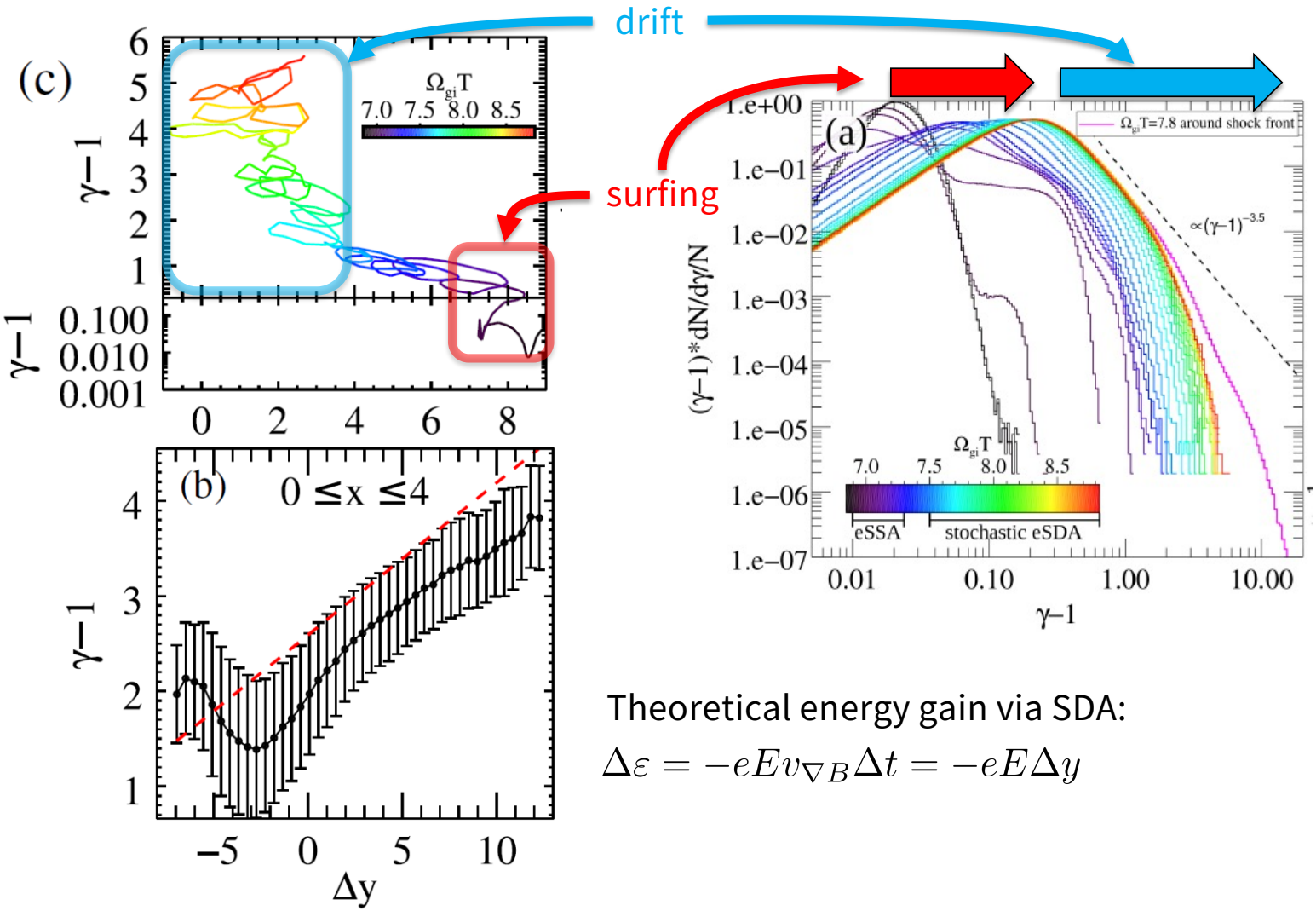

Theoretical energy gain via SDA:

$$\Delta\varepsilon = -eEv_{\nabla B}\Delta t = -eE\Delta y$$

3D PIC on the K computer (Matsumoto+2017, PRL)

Scattering by Weibel Turbulence

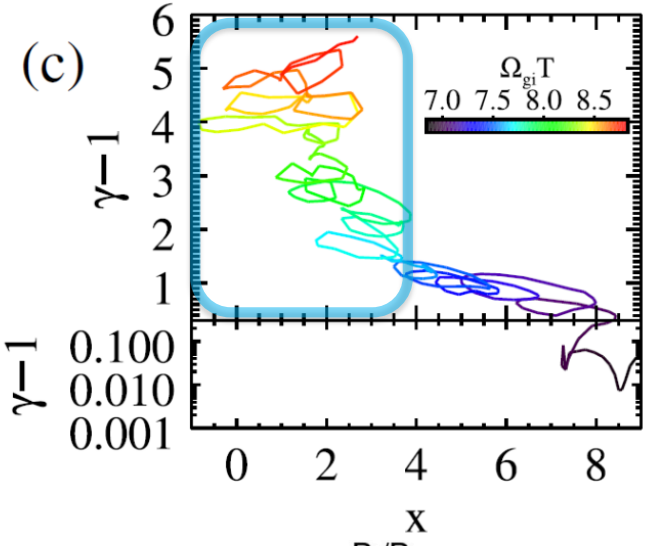

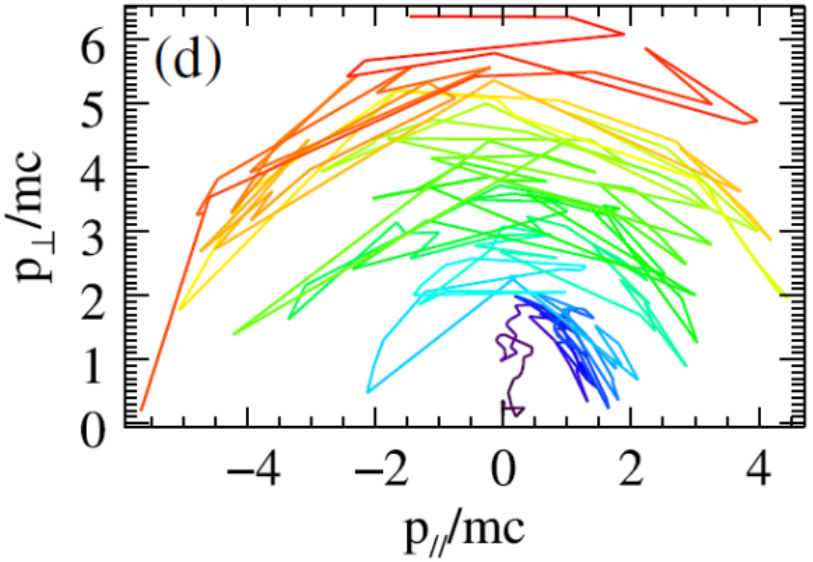

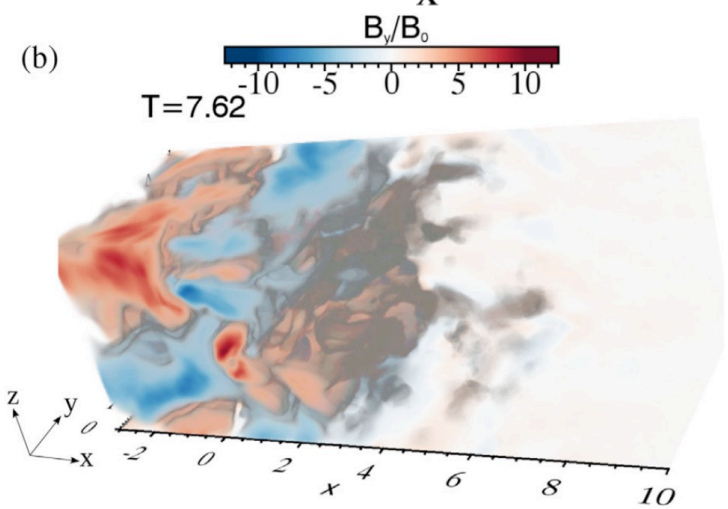

The strong Weibel turbulence play the role for the pitch-angle scattering.

More effective confinement of the particles in the acceleration region becomes possible.

Spontaneous Magnetic Reconnection of Weibel-Generated Magnetic field

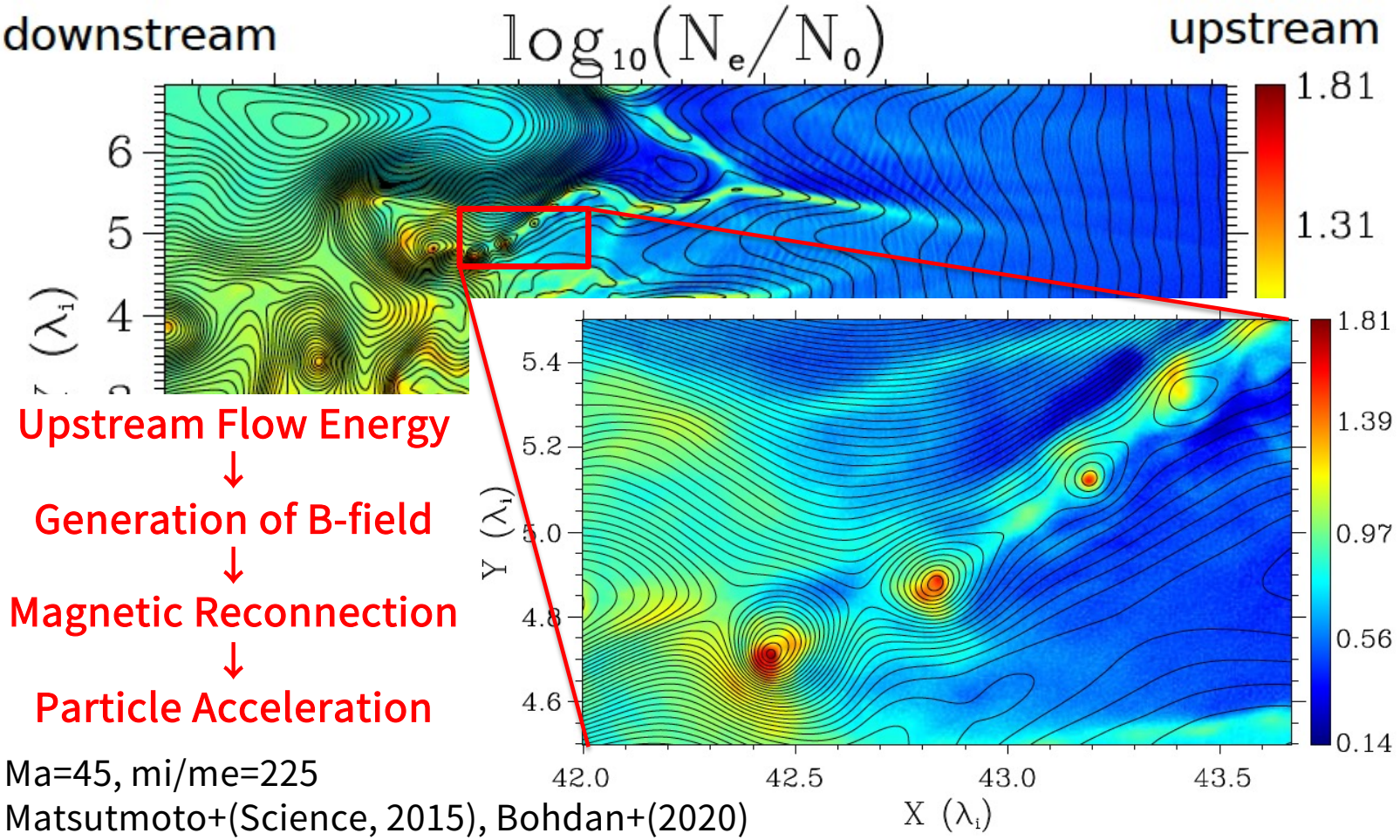

Upstream Flow Energy

↓

Generation of B-field

↓

Magnetic Reconnection

↓

Particle Acceleration

Ma=45, mi/me=225

Matsutmoto+(Science, 2015), Bohdan+(2020)

Nishigai & Amano 2021

Transition from Classical to Weibel-dominated shock

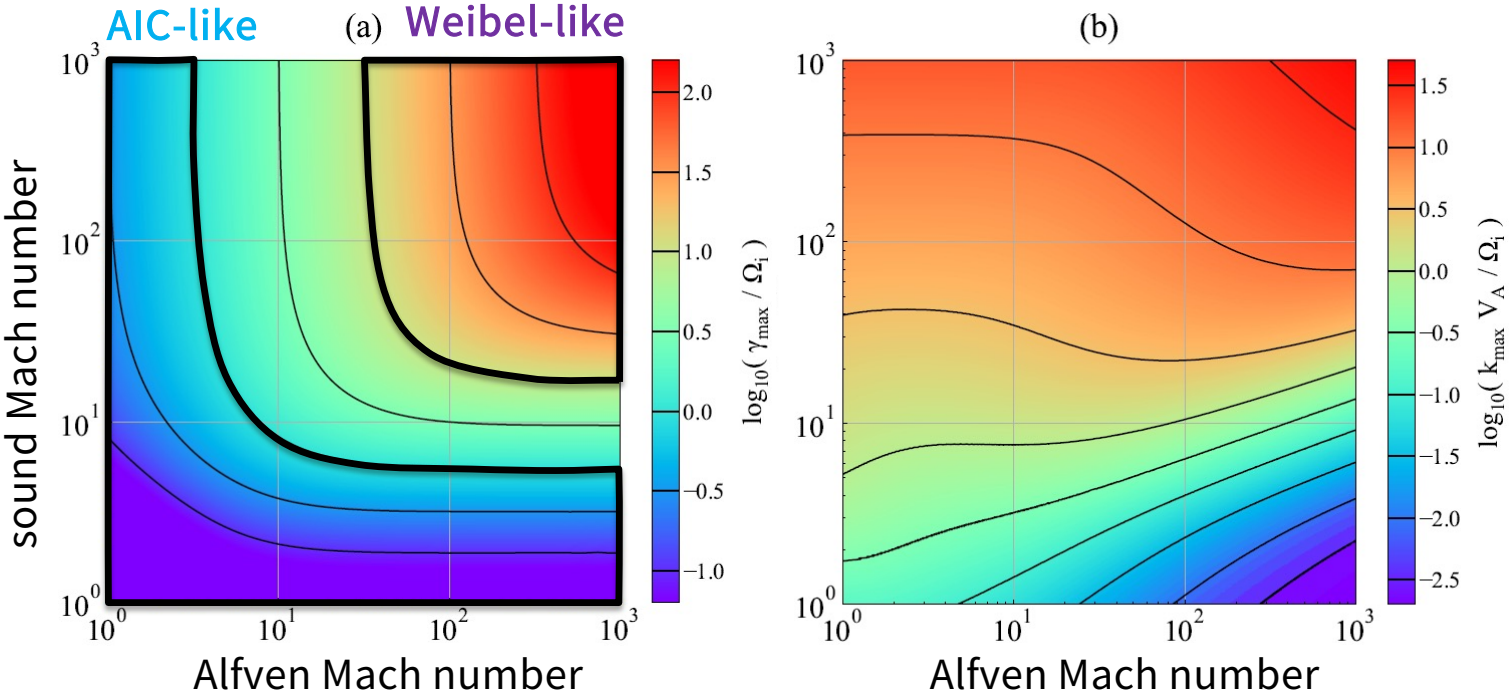

- The instability property transitions continuously from AIC ($\gamma/\Omega_i < 1$) at lower Mach numbers to Weibel ($\gamma/\Omega_i \gg 1$) regimes at higher Mach numbers.
- Typical bow shock parameters correspond to AIC-like (or rippling) instability, while young SNR shocks will likely be dominated by more violent Weibel-like instability.
- The Weibel-like instability might become dominant under exceptional solar wind conditions with very small magnetic fields and low temperatures. [c.f., Sundberg+2017, Madanian+2020]
- Efficiency and roles of magnetic reconnection are still uncertain. [Bohdan+2020]

Electron Acceleration Diagram

Saturn's bow shock [e.g., Masters+2013, 2016]

shock surfing (Buneman) + Weibel/Reconnection?
[e.g., Hoshino & Shimada 2002, Matsumoto+2015, 2017, Bohdan+2019]

high M_A

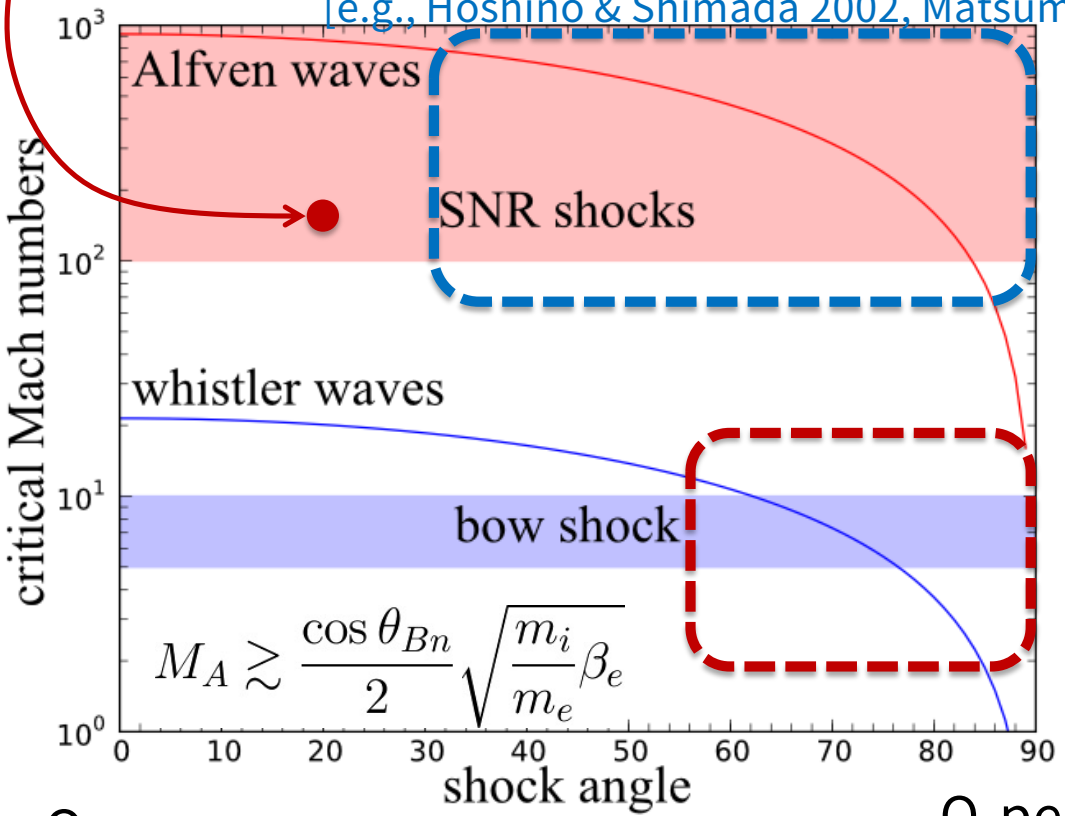

low M_A

Q-para

Q-perp

Earth's bow shock
[e.g., Oka+2006, Amano+2020]

intercluster shocks?

c.f., Amano & Hoshino 2010

結論

- 衝撃波電子加速問題の解決への道筋が（おぼろげながら）見えてきた.
- 拡散係数（散乱効率）が最も重要な量であると同時に最も大きな不定性でもある. ただし直接観測や数値シミュレーションで詰めていくことは可能.
- 別のアプローチ（レーザー実験・天文観測）も相補的に使える可能性あり.

Fiuza+2020 (Laser Experiments @ NIF)

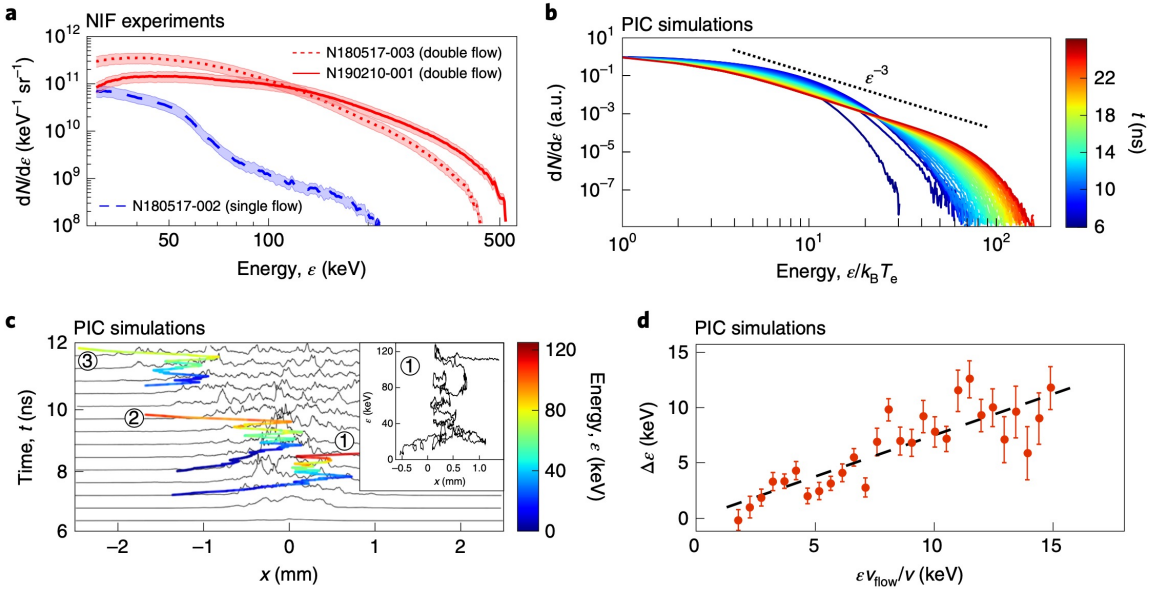

Tanaka+2018 (NuSTAR obs for W49B)